K O N I N K L IJ K N E D E R L A N D S
M E T E O R O L O G I S C H I N S T I T U U T

D e B i l t

WETENSCHAPPELIJK RAPPORT
W.R. 77-6

H.R.A. Wessels

A network of lightning counters in the Netherlands

De Bilt, 1977

Publikatienummer: K.N.M.I. W.R. 77-6 (MO)

U.D.C.: 551.508.94 :
551.509.1 :
551.594.21

A network of lightning counters in the Netherlands

H.R.A. Wessels

Summary

The design and the first results are described of a network of 18 lightning counters installed in the Netherlands by the Royal Netherlands Meteorological Institute (K.N.M.I.) during the years 1969-1973.

The main purpose of these counters is to determine the average number of lightning strokes to the ground per unit area and unit time.

The response of different types of lightning counters to the electric field change caused by idealized lightning strokes is treated in section 2. A slight preference is given to a sensitive instrument which responds predominantly to field variations with frequencies exceeding 3000 c/s.

The chosen instrument is described in section 3. Special attention is given to the comparability of the counters and therefore to the effects of earthing methods. Also the influence of nearby obstacles is investigated quantitatively. Arguments are presented to restrict the instrument to the detection of positive field changes exclusively: disturbance by point-discharge is avoided and misleading counts from distant winter storms are reduced.

To enable the quantitative application of these counters, methods for determining the "effective range" have been studied (section 4). Starting from an assumed log-normal amplitude distribution for the atmospherics the response of the counter to several simplified sources is derived. The (rare) occurrence of travelling isolated storms with constant flash rate as well as the passage of regular squall lines can be used to estimate the effective range.

A special group consists of storms that occur above the North Sea and the coastal region in autumn and winter. The effective range for discharges from these storms is appreciably larger than for warm season lightning: respectively about 70 and 10 km.

From these figures a first estimate of the average earth stroke density can be made: about two strokes per square kilometre per year.

A suitable division between warm-season and cold-season thunderstorms can be made at a 700 mbar temperature of -5 °C. This distinction is maintained throughout the report.

In section 5 a comparison is made between the "thunder heard" observing system and the counter results. Specific statistical criteria are proposed for the application of lightning counters as a replacement for observers.

Some first results of the network are presented in section 6. The registrations of the network on two occasions with severe hailstorms are discussed. Finally, a few climatological results for the years 1974-1976 are given. Many more of these counter results have been used as examples in other sections of the report.

Data from three years prove to be insufficient to draw conclusions on the existence or non-existence of so-called thunder nests. The large differences however between the diurnal and seasonal variation of the lightning occurrence at coastal respectively inland stations, could easily be demonstrated.

A few suggestions conclude the report.

-o-o-o-

Royal Netherlands Meteorological Institute,
Wilhelminalaan 10,
P.O. Box 201,
3730-AE-DE BILT.
Netherlands

Contents

1. INTRODUCTION

Lightning is studied for a variety of reasons, e.g.

- in relation to the protection of power lines, structures, etc.,
- possible disturbance caused to radio communications,
- for synoptic applications such as the long-range detection of low pressure centres.

Most observational material consists of: "the number of hours (or days) that thunder was heard". These observations are simple and more or less uniform throughout the world. The intensity of the thunderstorm however is not taken into account; more relevant data would be the number of flashes and their intensity. Moreover the advantages of the present method are gradually reduced by factors as the lack of observers, especially during the night, and an increased disturbance by noises of different origin.

Instruments have been designed to detect and even locate lightning. Locating is generally done by means of two or more direction-sensitive detectors at the far ends of a base-line. Another method uses three stations and computes the direction from the different times-of-arrival of spherics at these stations. There are also promising suggestions to achieve locating with a single station (Ruhnke, 1971).

In many countries and also in the Netherlands a less sophisticated solution has been chosen: to replace or complement the observers with a network of identical counters. Such counters are usually designed to be operated by the radio transmission of the lightning. They are composed of an aerial, a filter circuit and a triggering device that operates a recording unit. Electric field changes due to a nearby lightning are recorded if the induced voltage jump - after passing the filter - will exceed a certain preset level at the triggering device.

Individual characteristics of the numerous existing counter designs depend on the aerial configuration, the frequency response of the filter and the sensitivity of the triggering circuit. In addition, the counter can be designed to count exclusively either positive or negative field changes.

All this presents some degree of freedom to build counters with certain preferred properties, e.g. not to react on intracloud or intercloud lightning.

In the present report the design of the KNMI-counter is described and discussed in sections 2 and 3. In the following sections suggestions are worked out for a quantitative application of the network. Finally, a few examples are presented.

2. PRINCIPLES OF LIGHTNING DETECTION WITH SIMPLE RADIO EQUIPMENT

2.1 Average return-stroke parameters

Data on the magnitude of field changes caused by flashes of known location have only been published for a limited number of case-studies. More systematic observations have only been made recently, as part of a thorough study of thunderstorms in Florida that was initiated to protect the Apollo missions. See e.g. Tiller et al. (1976).

Relatively more data are available on the strokes themselves. Current measurements with magnetic links have been done since the last century and many other methods have been applied. It is therefore customary to compute the field changes resulting from a model flash, using thereby the more complete statistics that are available on return-stroke parameters.

Most earth strokes over flat country carry negative charge to the ground. From measurements with the Boys' camera the return-stroke channel is known to grow upwards from the ground with decreasing speed (Schonland et al., 1935). After a time t the length h of the channel of an average "model flash" may be given by

$$h(m) = h_o(1 - e^{-\gamma t}) \quad \text{with } h_o = 2400\ m \text{ and } \gamma = 30{,}000\ s^{-1} \qquad (1)$$

Uman et al. (1973) and also Leise and Taylor (1977) have argued that a transmission line model with a different return-stroke velocity profile should be used, especially for strokes within a range of a few kilometres. Because the model is mainly used here for a qualitative illustration, we follow equation (1).

The current i through the channel varies according to the well-known formula of Bruce and Golde (1941)

$$i = i_o (e^{-\alpha t} - e^{-\beta t}) \qquad (2)$$

With the exception of Müller-Hillebrand (1963) most authors assume the constants α and β to be independent of the value of i_o. The original figures used by Bruce and Golde are $\alpha = 44{,}000\ s^{-1}$ and $\beta = 460{,}000\ s^{-1}$. Norinder (cited by Uman, 1969, p. 122) has published examples of a stroke with a slower rate of rise of the current. Morrison (1953), Malan (1963, p. 100) and Croom (1964) discuss this discrepancy and the latter concludes that an average lightning stroke could be described with

$$\alpha = 10{,}000\ s^{-1} \quad \text{and} \quad \beta = 500{,}000\ s^{-1}$$

On the maximum current, reached at a time $t = \frac{1}{\beta - \alpha} \ln \frac{\beta}{\alpha}$, a large number of measurements is available. A log-normal frequency distribution for i_o with a median value of 22 kA, fits most of these measurements.

At this stage it should be stressed that no model stroke actually exists in nature. Systematic differences in the parameters α, β, γ, h_o and i_o can be expected for different seasons or regions. The problem is also complicated by the frequent occurrence of multiple discharges or strokes with reversed sign. Subsequent strokes - after the first return-stroke - seem to have a much faster rate of rise of the current (Tiller et al., 1976) and seem to reach to a larger height h_o as well.

2.2 Electric field change due to an idealized stroke to earth

With the numerical values suggested by Croom, the change with time of the current moment $M = 2\,i\,h$ of a typical return-stroke is known and the field change as a function of the distance r above a conducting earth is then given by electromagnetic theory (Israel II, 1961, p. 409-416)

$$E = \frac{1}{4\pi\varepsilon_o}\left(\frac{\int M dt}{r^3} + \frac{1}{cr^2}M + \frac{1}{c^2 r}\frac{dM}{dt}\right) \text{ Vm}^{-1} \qquad (3)$$

with $c = 3.10^8$ ms^{-1} and $\varepsilon_o = 8.85\ 10^{-12}$ Fm^{-1}.

A discussion on the limitations of (4) has been published by McLain and Uman (1971). In the above formula no account was given to the travelling time of the disturbance from the lightning channel to the observer.

Another item of interest is the frequency spectrum of the radiation transmitted by the stroke. From the preceding formula with Fourier-analysis: ($\omega = 2\pi\nu$)

$$E(\omega) = \frac{1}{4\pi\varepsilon_o}\left(\frac{1}{j\omega r^3} + \frac{1}{cr^2} + \frac{j\omega}{c^2 r}\right)\frac{2\,i_o h_o \gamma(\beta-\alpha)(\alpha+\beta+\gamma+2j\omega)}{(\alpha+j\omega)(\beta+j\omega)(\alpha+\gamma+j\omega)(\beta+\gamma+j\omega)} \qquad (4)$$

E(t) and the modulus of E(ω) are illustrated in the figures 1 and 2 for some values of the distance r from the discharge. Fig. 1 conforms very well with examples of measured field changes (Morrison, 1953, Tiller et al., 1976).

The first and last terms of (3) are commonly referred to as the electrostatic and radiative terms respectively. The radiative part of E is associated with the fast rise of E in fig. 1 in the first 3 μs. The electrostatic term is responsible for slow field changes lasting up to 200 μs. The contribution of this latter term decays rapidly with increasing r in contrast to the radiative part (r^{-3} compared to r^{-1}). Consequently, the frequency spectrum fig. 2 shows a more important role for the high frequency variations with increasing range. The contribution

of the second term, sometimes called the intermediate field, is only temporarily larger than the others. Fig. 3 illustrates the change of the field as a function of range for a counter with a low-frequency cut-off.

The frequency response of the antenna and the filter circuit determine how the counter will react on the field changes of fig. 1.

2.3 Frequency response of lightning counters

In networks of lightning counters two main types of equipment are used, sensitive to respectively fast and slow field changes:

- CCIR-counter. This is the best-known example of the first category. (CCIR = Comité Consultatif International des Radiocommunications). It is based on a design by Sullivan and Wells (1957). The choice of this counter has been recommended by the World Meteorological Organization (1959). The 3 dB pass-band is between 2 and 30 $kc.s^{-1}$ (Müller-Hillebrand, 1963). The CCIR-counter employs a vertical rod of 7 m in length as aerial. The triggering voltage at the antenna-entrance is 3 V.
- CIGRE-counter (Conférence Internationale des Grands Réseaux Electriques). This counter was originally designed by Pierce (1956). In later years many versions have been published including transistorized ones (e.g. Barham, 1965). The 3 dB transmission band of the filter is between 0.1 and 2 $kc.s^{-1}$. The aerial consists of a number of parallel horizontal wires at a height of 5 m. The triggering voltage normally used is 25 V.

Many publications have been devoted to the behaviour of both types of counters in several regions including the tropics. One of the objectives of such studies is the establishment of the "effective range r_e", relating the average ground flash density n in the region of the counter to the total number of flashes actually counted N_y in a certain period, e.g. a year.

$$N_y = \pi \cdot n \cdot r_e^2 \qquad (5)$$

The ground flash density n is the number of strokes to earth per square kilometre in a year. One of the main purposes of the network is the determination of n and to achieve this the value of r_e must be known. The formula (5) should be applied only for a series of observations with a constant value of n over the area concerned. It will be shown that the value of r_e depends on the type of thunderstorm. A long series of observations will be needed if we want to establish the average ground stroke density.

2.4 Comparison of two counter-types

Instruments that respond exclusively to the radiation component are not very suitable to establish the value of n. The counting range of the individual flashes will be proportional to $\frac{dM}{dt}$, and these counting ranges will have a considerable spread. The result is a large uncertainty in the estimate of r_e and, according to (5), an even worse result for n. This argument has favoured the development of the CIGRE-counter in contrast to the CCIR-counter. The spread of the counting-ranges is then reduced by the appearance of the third power of r. It should be stressed that part of the different behaviour of these counters can be explained by the lower sensitivity of the CIGRE-counter. It can be demonstrated with fig. 2 that a reduction of the counting-range to within 10 km by increasing the trigger-voltage would e.g. render a counter with a band-pass as high as 4 $kc.s^{-1}$ insensitive to the radiation component. Such a counter would then have the advantage of a well-defined effective range. The reverse would happen if a CIGRE-instrument were made more sensitive.

Cloud strokes may cause appreciable field-changes, especially at low frequencies.

A serious disadvantage of the low-frequency pass-band of the CIGRE-counter is the large percentage of cloud strokes included in the total count. Fractions of 50% are no exception. Some authors have suggested corrections to eliminate cloud discharges statistically (Prentice and Mackerras, 1969). These corrections use experimental values of the relative proportion of cloud flashes and also of the ratio of the effective ranges for cloud

respectively ground strokes. Accurate values of these factors are difficult to obtain: they depend on the type of thunderstorm and will therefore vary with locality and season and perhaps also from year to year. In the case of the CCIR-instrument the average proportion of cloud flashes counted is very small. If we use an insensitive version of the CCIR-counter (with an effective range comparable to that of the CIGRE-counter), the number of counted cloud strokes can be neglected.

The points of comparison listed so far present no decisive advantage for either of the counter-types. The calibration of both types is a difficult matter and will involve a large number of thunderstorms of all the types that occur in de region concerned.

Finally, a remark will be made on the polarity of the field-change. The slow field-changes become more and more negative for a distance larger than about 10 km. The value of E becomes even negative for large r ($\frac{dM}{dt}$ in equation (3) becomes negative after some time), and the total negative field-change will then exceed the preceding positive change. At the exit of the filter circuit we can then expect an increase of the relative magnitude of the slow negative voltage variations compared to the fast positive changes, due to the high-frequency cut-off properties of the filter. In the next section an application of this range-dependent phenomenon is suggested.

2.5 Important factors for the design of counter-networks

In setting up a network of these simple lightning counters, a choice has to be made of the sensitivity, the frequency response and the polarity of the counter. First of all this choice is determined by the purpose of the network. The following questions are relevant:

- Are cloud strokes to be measured (continuation of thunder-day records, thunderstorm warning) or to be excluded (determination of n) ? Is it possible to eliminate cloud discharges with a statistical procedure?

- The desired effective range has to be chosen, considering the number of instruments available and the possibility of installing stations. Is a full coverage necessary of the region concerned? This might be so for thunderstorm warning, but for study of e.g. the influence of local topography on thunderstorms, a counter with a very short range is to be preferred.

3. DESCRIPTION OF THE KNMI-NETWORK

(KNMI = Royal Netherlands Meteorological Institute)

3.1 General arrangements

A vertical aerial was chosen because of the lack of space at most locations and also to be certain of an equal sensitivity for all horizontal directions.

The electronics and the batteries are housed in a metal case fixed at the wooden pole that supports the aerial (fig. 4).

The circuit diagram of the counter is shown in fig. 5. The properties of the counter as sensitivity, frequency-range and polarity are to a large extent determined by the entrance components. The present design is intended to be flexible. If for some reason (e.g. international normalization) a change of the specifications would be necessary, this can probably be achieved by a minor change of components.

For the registration a mechanical ink-on-paper-tape printer (Sodeco, Genève, Suisse) is placed in the nearest building available with a mains connection. A timing device causes prints of the accumulated total to be made at ten-minute intervals, while after the last printing of each hour the counter is reset to zero. Therefore hourly counts can be read immediately from the paper-tape, but also the ten-minute sub-totals can be reconstructed from their cumulative registration. Synchronization of the respective counters is in principle provided for by the mains frequency. Because a power failure is not unlikely during thunderstorm situations, and because the printer may also become defective for other reasons, a separate battery-powered counter is placed in the instrument case. The latter counter presents only accumulated totals and serves as a back-up registration and as a permanent control.

3.2 Specifications of the instrument

The counter used in the network is essentially a transistorized CCIR-type of counter. The instrument has a low sensitivity (high triggering voltage) and responds to positive field-changes only. To avoid multiple counts (usually a lightning stroke consists of several individual return-strokes) and to protect the moving parts, the counter remains inoperable during 0.22 seconds after the triggering.

The entrance configuration is almost identical to the original CCIR-design except for different capacities of the aerial and its connection. The frequency response as shown with curve (a) in fig. 2 is between 5 and 70 $kc.s^{-1}$ (3dB points) and centred at 17 $kc.s^{-1}$.

The triggering voltage is set with a variable resistor at 15 V $\pm$ 0.1 V. The test-pulses are applied at the antenna-entrance. The aerial can remain connected during testing, if desired.

Some dependence of this preset sensitivity on temperature and supply-voltage could not be avoided. Tests demonstrated that in the range $-10^{o}C$ to $+40^{o}C$ temperature-errors did remain within $\pm$ 0.1 V (compared to the 15 V-level) if silicon-diodes were used.

Unfortunately, the triggering voltage is almost proportional to the supply voltage. The continuous current from the 6 V supply battery is about 0.2 mA, while a few thousands of counts per year of 0.2 s duration each, require an even smaller average current. Four large 1.5 V cells are used in series and an average reduction of 4% in the supply voltage ($\pm$ 2% = $\pm$ 0.3 V) can be expected if the batteries are replaced after a year. March and April are the best months to replace the batteries, so that the comparability of the counters is at its best during the main thunderstorm months in the Netherlands, namely May till September.

3.3 Sensitivity of lightning counters

In this category of devices the aerial is connected to earth by means of a filter circuit. As seen from the antenna base the impedance of the counter consists of a capacity C and a parallel resistor R (fig. 6). The aerial itself forms a capacity C_A with the earth.

The aerial is exposed to a constant field E. It acquires a charge Q from earth that can reach the aerial through the resistor R. We now suppose the external field E suddenly to disappear. At first the charge Q remains present in the condenser $C_A + C$. Of course the aerial will start to discharge with a time constant RC. From these considerations we find for the voltage at the antenna base

$$V = \frac{Q}{C_A + C} \; e^{-t/RC} \qquad (6)$$

The counter is calibrated to operate on test-pulses exceeding the threshold voltage V_t at the aerial entrance. These test-pulses are applied by discharging a condenser of 2.5 μF. These pulses contain all frequencies relevant to this instrument. The time RC is about 100 μs, i.e. much slower than most of the field changes discussed in the previous sections. The triggering field strength is related to the other instrument parameters by

$$Q(E_t) = (C_A + C)\, V_t \qquad (7)$$

C_A is derived in Appendix A. Q can be found by considering the aerial to be a vertically stretched ellipsoid, earthed with a thin wire (fig. 7). The ellipsoid receives such charge as to reduce to zero the potential at its surface. This potential is the result of adding the external field to the field of the charged body (Appendix A, (26))

$$-E z + \frac{Q}{4\pi\varepsilon_o} \; \frac{1}{2l} \left(\ln \frac{c+l}{c-l} - \ln \frac{2h+l}{2h-l} \right) \qquad (8)$$

where Q is found by putting this expression equal to zero for $z = h$. As it is impossible to fulfil this condition exactly, we should introduce here an effective height h_e of the aerial.

We substitute $a^2 = c^2 + l^2$, so $\ln \frac{c+l}{c-l} = 2 \ln \frac{c+l}{a}$. For a thin rod we take $c = l$, and find

$$Q = E.h_e \; \frac{2\pi\varepsilon_o \cdot 2l}{\ln \frac{2l}{a} - \frac{1}{2} \ln \frac{2h+l}{2h-l}} = E.h_e.C_A \qquad (9)$$

Combining this with (6) results in the following expression for the threshold field-strength of a lightning counter with an elevated thin vertical aerial

$$E_t = \frac{V_t}{h}\left(1 + \frac{C}{C_A}\right) \qquad (10)$$

Substituting some data from fig. 4 and 5: h = 3.5 m, ℓ = 1.5 m, V_t = 15 V, we find the triggering field-strengh of the KNMI-counter E_t = 40 V/m for C = 230 pF including the capacity of the cylinder at the antenna-base, the capacity of the co-axial cable and the effective capacity of the filter as seen from the antenna-entrance. The latter capacity is decreasing for higher frequencies, so the sensitivity of the counter is a little higher for distant discharges.

3.4 Influence of obstacles on the counter-calibration

At all stations the same sensitivity is maintained. In order to make comparisons between counters at different stations meaningful, a few conditions must be met. Firstly, the type of thunderstorms at both stations should be comparable, at least statistically. Secondly, not only the instruments should be identical, but also their positioning with respect to the surroundings. Two sources of error are apparent: a shielding of the electrical field by obstacles, and also differences in the earth-connection at various locations.

In the literature no references could be found concerning the influence of obstacles like trees, buildings, etc. on the field-strength caused by a lightning-stroke. A reasonable estimate, based on potential theory, of the errors to be expected from objects of different size and shape is presented in Appendix B. A verification of these results should be possible by comparing an undisturbed counter with a neighbouring counter under the influence of a well-defined obstacle. Such an experiment, however, has not yet been carried out. Small-scale tank experiments have been published by Bogner and Conners (1967). Their results are in agreement with Appendix B if comparable objects are considered.

Some experimental information on the weakening of an actual VLF radio transmission near to vertical conducting poles has been presented by Kikushi and Araki (1972). Their results point to a more serious disturbance than can be derived from Appendix B. A distant ground-based transmitter and a lightning flash are naturally quite different sources. For taking decisions on obstacle-clearance a conservative application of Appendix B seems advisable. An extreme example of the influence of obstacles has been a counter located at Witteveen during some years before 1973. The counter was partly surrounded by trees up to 8 m high at ranges between 7 and 15 m from the counter and the result was a reduction of the count to about 30% of what could be expected from neighbouring stations.

3.5 Influence of earthing on the calibration

The circuit-earth is connected to a vertical rod of 2 m (fig. 4). In addtion, a small "ground plane" is used consisting of six wires (2 m in length) laid radially from the top of the earth rod.

The soil around these conductors can be wet as well as dry and it is important to know whether this has any influence on the counter's sensitivity. Experiments have been performed at the observing field of the central office of the KNMI at De Bilt to compare counters having various earth connections.

These tests were carried out from mid-1972 until mid-1973. The prototype counters used at the time were sensitive to positive as well as to negative field-changes with a threshold of about 15 V. A counter with a complete earthing according to fig. 4 was compared with another counter of which successively the earth rod, the horizontal threads and finally both had been disconnected. Each comparison involved hundreds of registered lightnings.

All differences between the simultaneous counts could be attributed to small differences in (positive or negative) sensitivity except for the last - rather rigorous - modification, which caused about 20% of the counts to be missed. An earth connection with either the six pins or the earth rod proved as efficient as

the combination of both, i.e. a counting error could not be detected and must have been smaller than 1%.

This applies however to the complete series of measurements, during most of which the soil must have been wet due to nearby thunderstorms. To be certain that the counter will also be operating at e.g. the end of a long dry period, the combined earthing of fig. 4 is recommended.

3.6 An independent test on the comparability of counters

During some situations flashes occur that can trigger these counters at ranges up to 200 km. In section 5 more attention is given to this phenomenon. Inspection of simultaneous counts can inform us whether some counters failed to work while others did register a stroke at the same or at a greater range. Of course the location of the flash must be known, e.g. with the help of radar or thunder reports.

It should be mentioned that propagation influences can be important at such ranges (Uman et al., 1976), especially if large water-surfaces have to be crossed. Frequencies of 100 kc/s or more will then be attenuated.

In a limited number of cases this test was used for the present network. All counters did operate as could be expected. It is recommended to repeat these tests in the future, because they are very suitable as an independent control of the network.

3.7 Elimination of false counts caused by point-discharge currents

A prototype counter has been operating at Vlissingen (Flushing) at the North Sea coast (see fig. 11) since July 1971. With this counter counts of up to hundreds per 10 minutes could occur even in the absence of thunderstorms! This disturbance was caused by the so-called point-discharge or corona current that flows into or out of sharp elevated points in the presence of strong electric fields.

In many cases it is possible to distinguish the unrealistic high counts caused by corona from thunderstorm counts. It is however better to avoid a disturbance altogether than to eliminate its effects with e.g. a statistical criterium that will fail in some individual cases.

The round top of the aerial that had been introduced already at the first prototype was meant to reduce the field strength near the top of the aerial. Point-discharge effects were not sufficiently eliminated.

To overcome these difficulties attention was given to the differences in occurrence and behaviour of corona currents in positive respectively negative fields. Conventionally, positive corona occurs in positive fields (potential increasing upwards). The current flows into the point which remains negatively charged. Large and Pierce (1955) demonstrated the different behaviour of corona in positive fields, consisting of fast regular "Trichel-pulses", and in negative fields, being a continuous current with superimposed isolated bursts. Positive corona is probably more usual during the wintery coastal showers that on most occasions accompany this phenomenon. Finally, it is known that positive corona starts at a lower absolute value of the field strength (Chalmers, 1967).

It was therefore decided to discriminate the count in terms of the polarity of the field. In November 1973, a separate counter, sensitive only to positive field changes, was placed in the neighbourhood of the original counter at Vlissingen. The results of the comparison were very encouraging. In the test period, when 21 improbably high hourly totals occurred at the first counter, no corona was noticed at the modified counter! (fig. 8). This advantage was gained without diminishing the counter's performance as a lightning detector.

As a result of this and because of the arguments from the next paragraph it was decided to modify all the counters to positive field-change detection. Since then the occurrence of disturbing corona currents has become a rare phenomenon (fig. 9). All the cases from 1974 onwards could easily be recognized by a sudden unrealistic rise of the counting rate.

It is perhaps interesting to note that point-discharge most frequently occurs at coastal stations during autumn and winter storms. These storms are favoured by the relatively warm North Sea water and are quite often accompanied by wet snow or small

hail. Another factor making point-discharge easier is the free exposure of the aerial to surrounding trees. This has apparently an influence on some stations.

Finally, it should be mentioned that no definite explanation could be given of the positive counter being insensitive to positive corona. A possibility could be that the Trichel-pulses are too fast to pass through the filter-circuit with sufficient amplitude. Special measurements would be needed to confirm this.

3.8 Further comparison between counters of different polarity

From the analysis of a model flash the suggestion followed (2.4) to avoid counts from distant strokes by restricting the polarity of the counter to positive field-change only.

This idea was tested empirically at De Bilt during the period 1973, May 15 till 1973, October 30. Three counters were used at the same time, one as the prototype and two being insensitive to respectively positive and negative pulses. Unfortunately, the positive thresholds were a little higher than the negative ones (+15.3 V compared to -13.8 V). Also the temperature-coefficient of the negative threshold is appreciable in contrast to the positive threshold (see 3.2).

The results of this comparison are summarized in Table 1. The classification with respect to the upper-air-temperature ($T_{700(mbar)}$ from the relevant sounding at De Bilt)was chosen to distinguish between summer-type and winter-type thunderstorms. It is a readily available parameter related to the height of the $0^{o}C$-level and therefore also to the height of the main charge centres of a thundercloud.

Apparently there is a rather sharp distinction between thunderstorms typical of the summer months and those in a colder air mass. For the first type the $\pm$ and + counters reach the same totals. The remaining small difference is probably caused by a small difference in sensitivity. It should also be remarked that the equality of the totals does not prove that the counts were registered simultaneously. A more detailed analysis shows however

Table 1 Number of counts by instruments with different polarity.

T_{700}(°C)	3°C-classes centered at:	-16	-13	-10	-7	-4	-1	+2	+5 °C
number of days with counts		1		3	7	9	11	4	1
number of counts on counters	+	27		29	43	363	64	57	28
	±	54		56	75	363	77	58	18
	-	63		54	77	181	65	32	1

that at least 90% consists of simultaneous counts of the same stroke on the two counters.

For nearby lightning the negative field-changes are normally absent as can be expected from e.g. fig. 1. Triggering does occur from various ranges and the net result is that only about 50% of the strokes in the warm group that are counted because of positive field jumps do also have strong enough negative field-change components within the same atmospheric.

The reverse is true for storms of the cold group. Strong positive field-changes become relatively more rare.

The comparison at De Bilt between two counters (positive + negative and positive) was extended beyond the period referred to in the beginning of this paragraph. The results obtained during 1973 are illustrated in fig. 10. Again, the material was split into days with a 700 mbar-temperature respectively lower than and equal to or above -5°C. Notably in the cold group the number of "false alarms" is greatly reduced: a count rate exceeding 3 per hour in the absence of thunder and therefore of a thunderstorm within the nearest 10 km.

From the three prototypes considered here, the counter for positive jumps has the most desirable properties: counts from outside the effective range are suppressed in comparison to the other instruments. This advantage is most striking during the cold season. Since early 1974 all counters are modified accordingly.

3.9 Location of stations

The following restrictions had to be taken into account in the choice of stations for the network:

a. only 20 counters would be available;
b. preference should be given to existing hourly reporting "synoptic" stations;
c. the counters should together form a more or less regular grid.

Because of the condition sub b. 12 out of 18 counters are located at synoptic observing stations, and the gaps were filled in a regular way with two existing rainfall stations and four new stations. The stations (with their international code numbers) are presented in fig. 11. The coverage of the network would improve by placing stations near the open circles in the figure. This completion has been postponed due to a lack of spare parts.

The regularity of the grid would also improve by shifting some stations in the southwest to a location 10 or 20 km to the north. At some stations the situation of the counter is not ideal, especially because of surrounding obstacles. The value of the records for climatological purposes can diminish by changes in the surroundings. It is probably inevitable that in the future removals will be necessary.

With the existing stations 100% of the land surface of the Netherlands is within 30 km from a lightning counter, whereas 65% of that area is within 20 km.

4. ESTIMATION OF LIGHTNING STROKE DENSITY

4.1 Introduction

The application of lightning counters for measuring n, the number of flashes to earth per unit area in a certain period, can be reduced to the determination of the effective range of the counter as defined in section 2.3:

$$N_y = \pi \cdot n \cdot r_e^2 \qquad (5)$$

Regional and seasonal influences may result in a different value of r_e. It is therefore important to find values of r_e for different types of thunderstorms.

The calibration of the counter can generally be carried out by establishing the fraction P(r) of all earth flashes that are actually counted in dependence on the distance from the counter. Some authors (Prentice and Mackerras, 1969) call P(r) the performance curve of the counter. After integrating P(r) we can solve r_e from (5):

$$N_y = 2\pi n \int_0^{\infty} r.P(r)\, dr \qquad (11)$$

The same remark as to regional and seasonal differences in r_e applies to P(r). A serious limitation is further the implicit assumption of a homogeneous distribution for n. Notably for the autumn showers that occur along the Netherlands coast this is not realistic.

In the following paragraphs possibilities to evaluate $P_t(r)$ (t for a certain type of storm) are investigated. In order to find P(r) we need counter results, but also the real flash-rate of the sources and their locations. For the present investigation no separate measuring system to obtain this information was available. The use of visual observations to achieve this, has been reported by Boer (1967).

Only in some special cases - a minority of the storms - the problem can be tackled with the available means. An isolated

thunderstorm e.g. can be tracked by radar, and P(r) can then be determined if we suppose a constant production of flashes. Examples follow in section 4.8.

First of all however the properties of an analytic approximation for P(r) will be investigated.

4.2 Probability of field-change amplitudes

In section 2.2 approximate values were derived for the field-change E(r) detected by a counter with a certain frequency response after the occurrence of an average return stroke at a distance r. In section 3.3 the triggering field strength E_t of the KNMI-counter was derived.

If all earth strokes would cause the same field change, the limiting triggering distance could easily be solved from $E(r) = E_t$. With this simplification we have $r = r_e$ and n would follow from the total count during a long period.

A more realistic approximation has been proposed by Horner (1960). A lognormal distribution of E-values is used and the field strength for an individual stroke is supposed to decrease with r^{-m}. The lognormal E-distribution is more or less justified by series of observed lightning currents (e.g. Frühauf et al., 1966). The method neglects of course the (probably small) amount of very weak earth strokes not included in the statistics!

The probability of E exceeding the triggering field strength E_t is then given by

$$P(r) = \frac{1}{\sqrt{2\pi}} \int_{\frac{\log E_t/E_d}{\sigma}}^{\infty} e^{-\frac{1}{2}u^2} du \qquad (12)$$

σ is the standard deviation of the distribution of $\log \frac{E}{E_d}$, while E_d is the median value of E at a range r. The range-dependence of E_d is as follows

$$\log \frac{E_d(r)}{E_d(r_o)} = - m \log \frac{r}{r_o} \qquad (13)$$

We introduce the range r_d at which a median stroke E_d can just trigger the counter:

$$\left(\frac{r_d}{r_o}\right)^{-m} = \frac{E_t}{E_d(r_o)} \qquad (14)$$

Evidently for $r = r_d$ we have $P = \frac{1}{2}$ and (12) becomes

$$P(r) = \frac{1}{\sqrt{2\pi}} \int_{\frac{m}{\sigma}\log\frac{r}{r_d}}^{\infty} e^{-\frac{1}{2}u^2}\, du \qquad (15)$$

4.3 Probability of counting strokes at a certain range

For practical reasons we want to normalize the range with respect to the effective range r_e. From (5) and (11)

$$\pi r_e^2 = \int_0^{\infty} P(r).\, 2\pi r\, dr \qquad (16)$$

Carrying out the integration with (15) and taking $\log \frac{r}{r_d}$ as a new variable

$$r_e^2 = \frac{2\, r_d^2\, \ln 10}{\sqrt{2\pi}} \int_{-\infty}^{\infty} e^{2\log\frac{r}{r_d}\ln 10}\, d\log\frac{r}{r_d} \int_{\frac{m}{\sigma}\log\frac{r}{r_d}}^{\infty} e^{-\frac{1}{2}u^2}\, du$$

If we change the boundaries of the integration

$$r_e^2 = \frac{2\, r_d^2\, \ln 10}{\sqrt{2\pi}} \int_{-\infty}^{\infty} e^{-\frac{1}{2}u^2}\, du \int_{-\infty}^{\frac{u\sigma}{m}} e^{2\log\frac{r}{r_d}\ln 10}\, d\log\frac{r}{r_d}$$

$$= \frac{r_d^2}{\sqrt{2\pi}} \int_{-\infty}^{\infty} e^{-\frac{1}{2}u^2 + 2\frac{u\sigma}{m}\ln 10}\, du$$

Introducing $u = \frac{2\sigma \ln 10}{m}$ as a new variable, we get the solution

$$r_e^2 = r_d^2 \, e^{\frac{2\sigma^2 \ln 10}{m^2}} \quad \text{or}$$

$$\frac{r_e}{r_d} = e^{\frac{\sigma^2 \ln^2 10}{m^2}} \tag{17}$$

It is interesting to note the appearance of a single parameter $\frac{\sigma}{m}$. Some values for (17) are given in Table 2.

Table 2 Relations for the effective range.

m/σ	2	3	4	6	8
r_e/r_d	3.73	1.80	1.40	1.16	1.09

σ can be estimated from field-change measurements in the literature. Typical values are between 0.25 and 0.50 (resp. 5 and 10 dB). From section 2 we know m to be between 1 and 3, for a radiation field-counter probably below 2. The value of $\frac{m}{\sigma}$ is not independent of range as was supposed in the derivation of (17)! Fig. 3 gives a sketch of the range-dependence of m.

(17) can be used to rewrite (15)

$$P(r) = \frac{1}{\sqrt{2\pi}} \int_{\frac{m}{\sigma} \log \frac{r}{r_e} + \frac{\sigma \ln 10}{m}}^{\infty} e^{-\frac{1}{2}u^2} \, du \tag{18}$$

This equation is illustrated in fig. 12. In addition, fig. 13 presents the distribution with respect to distance of the pulses actually triggering the counter. The original distribution of the sources has then to be homogeneous. For $\frac{m}{\sigma} = 8$ most of the flashes counted come from just within the effective range-circle. Only 23% of all counts come from outside this circle in contrast with 74% for $\frac{m}{\sigma} = 2$.

4.4 Comparing total counts obtained at different sensitivities

With the present statistical atmospherics model (12) we can investigate how the total count varies if E_t is changed to E_t'.

From (14) and (17) the ratio of the effective ranges is found

$$\frac{r_e}{r_e'} = \left(\frac{E_t}{E_t'}\right)^{1/m} \tag{19}$$

and with the definition of r_e

$$\frac{N'}{N} = \left(\frac{E_t}{E_t'}\right)^{2/m} \tag{20}$$

Again, the main simplification is the use of a range-independent m. The flashes included in N' will be at a larger average range than those of N if $E_t' < E_t$. The relevant m-value is therefore different for these counters. Another problem is the inhomogeneous distribution of strokes over a larger area. From the records obtained so far in the Netherlands it seems that the strokes are unevenly distributed even in samples of a year or more. This is mainly caused by the large contribution of a few heavy showers.

From 1974, April 23 till 1975, June 10 an extra counter was in operation at De Bilt, using a trigger level of 8.3 V. So $\frac{E_t}{E_t'} = 1.8$. In fig. 14 daily totals of both counters are compared and also lines representing (20) are drawn. 32 days are not included, because there was no count at the regular counter and logarithmic scales are used. On separate days the distribution of strokes could be very different: an isolated storm within the effective range of both counters would result in almost equal counts. On the contrary, a storm can pass just within reach of the sensitive counter but too far from the other. Two extreme dates are marked in fig. 14. More details of these dates are given in later sections (1974, Sep. 15 and Aug. 17).

From fig. 14 it is difficult to estimate m. For low counts (distant storms) the points cluster with an appreciable spread

around the line m = 1.0. This is not surprising in view of the results of section 2 (e.g. fig. 3). The data included in fig. 12 do not suggest any relationship of m with the upper air temperatures.

A number of days has been selected with a more or less uniform distribution of strokes. The counts of six counters surrounding De Bilt were used as a control for this uniformity. For this selection of days $m \backsim 1.2$ was found as average value. This result can be useful e.g. to correct for small errors in E_t.

4.5 Comparing counters of different sensitivity in dependence on range

A more direct application of simultaneous counts with different trigger levels has been presented by Müller-Hillebrand (1963). He regarded the ratio of the counting rate at both instruments as a function of the distance from the stroke. In the present notation:

$$\frac{P(r)}{P'(r)} = \frac{\int_{\frac{m}{\sigma}\log\frac{r}{r_e}+\frac{\sigma \ln 10}{m}}^{\sim} e^{-\frac{1}{2}u^2}\,du}{\int_{\frac{m}{\sigma}\log\frac{r}{r_e}+\frac{\sigma\ln 10}{m}-\frac{1}{\sigma}\log\frac{E_t}{E'_t}}^{\sim} e^{-\frac{1}{2}u^2}\,du} \qquad (21)$$

Curves illustrating this ratio are given in fig. 15 for $\frac{E_t}{E'_t} = 1.8$, the value used during the test at De Bilt.

If the position of an isolated point-source is known, this graph can be used to find r_e. Unfortunately, the accuracy of the result will be rather low, due to the uncertainty regarding σ. The method can probably be useful if the ratio of the counts is about 0.6, which occurs for sources at a range of about 0.85 r_e.

The graph can also be used for a moving thunderstorm passing near the station. The advantage over the single counter is that

no stationary flash-rate has to be assumed as in the next section. The application remains subject to the restriction that the amplitude-distribution of the atmospherics is constant with time.

A suitable procedure is to plot the observed $\frac{P(r)}{P'(r)}$ against log r and then use fig. 15 as an overlay. The σ-curve with the best fit (take e.g. m = 1.2) can be found by shifting along the abscissa. In this way r_e and σ can be estimated. The desired model-situation did however not occur among the thunderstorms in the period of simultaneous counts (1974-1975). The cells should be small compared to r_e, but long-lived enough to travel at least a distance 2 r'_e, whereas during the measurements no other cell should cause registrations at the most sensitive counter. All this seems hard to fulfil.

Since April 1975 the extra counter at De Bilt has been dismantled, so the described method was not applied during the present study.

4.6 Counting-rate near specified sources of atmospherics

Fig. 12 is the counting-rate as a function of distance from a point-source matching the assumptions discussed in 4.1. These curves can also be used in reverse to estimate $\frac{m}{\sigma}$ and r_e for a certain case if the counting-rate is known for various distances from the source.

Curves like fig. 12 can be constructed in two types of situations:

a. If r_e is comparable to the station-spacing of the network, we can use the counts from many stations at various ranges from the thunderstorm. Of course this would not work in the presence of active sources at other locations.

b. If a stationary point-source is moving with monotonous speed, the range is known as a function of time. The time-dependence of the counting-rate can then be transferred to the desired graph.

Especially with the last method some difficulty may arise if thunderstorm cells are not small with respect to r_e. To get a first idea of the effect of broadening a source, fig. 16 was

constructed to present the total effect of five sources, respectively at the centre and at the corners of a square with diagonal r_e. Such a shape is probably as realistic as e.g. a circular area. The result is very encouraging: differences due to the spread in lightning parameters and to propagation characteristics are smoothed out at close range. We can conclude that a stationary shower passing overhead will produce about 40% of the maximum counting-rate at a distance r_e.

Thunderstorms will seldom pass exactly overhead and therefore in fig. 17 the results are given for respectively a point-source and for the configuration of fig. 16, passing both at a distance $\frac{1}{2} r_e$ from the station. The distance r has now to be replaced by x, measured from the point on the storm track closest to the counter. For the point-source the counting-rate decreases to 40% at $x = 0.85\ r_e$, while the curves for the broadened source are nearly the same as for fig. 16.

It is concluded that the recordings of thunderstorms producing lightning at a constant rate and moving with constant speed can be used to estimate r_e if they pass near the station.

4.7 Counting near line-sources of atmospherics

Quite frequently thunderstorms are not isolated but organized in squall-lines or fronts. We therefore suppose a narrow line-source to pass over the station. Introducing the coordinates x and y as in fig. 18, the counting-rate relative to its maximum for $x = 0$ is given by:

$$P(x) = \frac{\frac{2}{\sqrt{2\pi}} \int_0^{\infty} \frac{dy}{r_e} \int_{\frac{m}{\sigma} \log \frac{\sqrt{y^2+x^2}}{r_e}}^{\infty} e^{-\frac{1}{2}u^2}}{\frac{2}{\sqrt{2\pi}} \int_0^{\infty} \frac{dy}{r_e} \int_{\frac{m}{\sigma} \log \frac{y}{r_e}}^{\infty} e^{-\frac{1}{2}u^2}} =$$

$$P(x) = \frac{\displaystyle\int_{\frac{m}{\sigma}\log\frac{x}{r_e}}^{\sim} e^{-\frac{1}{2}u^2}\sqrt{10^{2\frac{\sigma}{m}u^2} - \frac{x^2}{r_e^2}}\,du}{\displaystyle\int_{0}^{\sim} e^{-\frac{1}{2}u^2}\cdot 10^{\frac{\sigma}{m}u}\,du}$$

$$P(x) = e^{-\frac{1}{2}(\ln 10)^2\frac{\sigma^2}{m^2}} \int_{\frac{m}{\sigma}\log\frac{x}{r_e}}^{\sim} e^{-\frac{1}{2}u^2}\cdot\sqrt{10^{2\frac{\sigma}{m}u} - \left(\frac{x}{r_e}\right)^2}\,du \qquad (22)$$

This integral has been solved numerically and the results are presented in fig. 18. The crossing of all curves for $x = 0.8\ r_e$ provides another criterium for estimating r_e. It is also of interest to note the resemblance with the dashed lines of fig. 17 for the displaced point-source. This suggests that these curves also apply to an interrupted line-source.

Apart from stationarity the demand for a narrow line is hard to fulfil. Therefore the result for two parallel lines at a mutual distance $\frac{1}{2}\ r_e$ has also been sketched in fig. 18. The curve for $\frac{m}{\sigma} = 4$ more or less coincides with the curves of fig. 16. It should be mentioned that Frühauf et al. (1966) treated the problem of the line-source in a rather similar way: starting numerically from (12) instead of (22). They state that the influence of widening the line to 2.25 km (about 13% of their r_e) can be neglected.

From these simple models it is evident that the stretching or displacing of the sources perpendicularly to the direction of translation is favourable for the determination of r_e, in contrast to the broadening along that direction.

4.8 Determination of the effective range using only one counter

In fig. 16-18 it has been demonstrated that showers passing nearby or storms arranged in lines do reach about 40% of their counting-rate at a distance $x = r_e$. This also applies to narrow line-sources.

The 10-min. printing interval prohibits the detection of rapid changes of counting-rate. Most storms last half an hour or more and the 10-min. counts generally give an adequate description of the rise and decline of the counting. For this purpose a 5-min. print would probably have been more suitable at the cost of a more time-consuming analysis of the records. For an accurate determination of the curves it is necessary that the maximum flash-rate should be rather high (3 per minute or so). This limits the number of cases suitable for this type of study. The best storms that occurred during 1974 till 1976 are illustrated in fig. 19 and tabulated in Table 3.

The data concerning the paths of the storms and their stationarity have been obtained from hourly radar sketches and from daily measurements with a dense precipitation network. The flash-rates of fig. 19 were plotted cumulatively and the time-difference between reaching 20% and 80% of the total has been converted to the value of r_e appearing in the last column.

Table 3 Isolated storms suitable for the determination of r_e

date	time gmt	station	estimated passing distance(km)	stationarity	speed km/hr	r_e (km)
1974 Aug. 4	1716	Lelystad	< 2	max. near station	48	7
4	1914	Heemskerk	3		63	12
17	0246	Volkel	4	max. later	80	13
Sep. 12	2318	Heemskerk	< 2	same storm	66	11
13	0040	Lemmer	5	same storm	66	10
15	1601	De Bilt	< 2	max. near station	39	5.5
1975 May 7	1638	Raalte	< 2	starting near station	60	6
1976 Sep. 29	1106	Raalte	5		44	8
29	2020	Lemmer	3		34	9

The spread in the resulting r_e-values is quite large. As can be expected, a low flash-rate near the station will lead to an overestimate of r_e (1974 Aug. 17), while too low values for r_e are found for short-living showers (1974 Sep. 15). In the latter example an analysis of the simultaneous registration of the sensitive counter at De Bilt (4.4) resulted in $r_e' = 6.6$ km. With (19) (actually based on a homogeneous distribution of sources) we would find $m = 3.0$. This value is incredibly high, so it can be concluded that r_e' is underestimated and probably also r_e.

From the more trustworthy cases in Table 3 the average result is $r_e = 10 \text{ km} \pm 2 \text{ km}$. The estimated accuracy of 20% corresponds to a 40% uncertainty in N-values (6).

The examples in Table 3 are typical of moderately active travelling thunderstorm cells. These are not uncommon during the summer season. The radar-tops were between 8 and 10½ km. 700 mbar temperatures in these situations ranged between -3 and +4 °C. No connection between these values and r_e could be found for this small sample of inaccurate r_e-estimates.

The conclusions from these measurements are encouraging but not fully satisfactory. It is advisable to repeat these tests with suitable storms that will undoubtedly occur in the coming years. Suitable storms are small, fast-moving and produce lightning at a high and constant rate. They also must pass within a few kilometres from a counter.

4.9 The use of simultaneous registrations by two or more counters

(Example a of 4.6). With large r_e, all the counters within circles around the source are triggered. From an analysis of the radii of these circles the curve P(r) can be found.

Although 10-min. counts are not ideal to prove simultaneity, the low count-rates during situations with large r_e make it easy to accept simultaneity if neighbouring stations count the same number in corresponding time-intervals. In many situations the only registration during some hours will occur on two or more counters in the same 10-min. interval.

These cases are rare in the summer season, but occur quite frequently with cold-air lightning. As mentioned in section 3.8 such storms are typical of the coastal region during the autumn. Lightning strokes from storms over the North Sea are often capable of triggering inland stations. On some (rare) occasions the whole of the present network was triggered by a lightning stroke over the North Sea. This is indicative of field changes exceeding 40 V/m at a range of 200 km!

Although the flash-rate is lower in these storms, the larger triggering-range can create the impression that autumn storms are electrically more active than summer thunderstorms (Horner, 1967). Large field-changes near winter thunderstorms have also been found by others. Takeuti et al. (1973) report 4000 V/m at a distance of 10 km from such a storm in Japan.

Examples of the distribution of total counts are given in fig. 20 and 21. For some days the P(r) curve has been found in the described manner with the help of radar and volunteer thunder observations to locate the sources (fig. 22). The vertical scale used is X.P(r) to indicate that an unknown percentage of the weaker strokes will have been missed by the network. The maximum flash-rate is probably occurring over the North Sea and is therefore unknown. The curve for December 4 in fig. 22 could be fitted with the $\frac{m}{\sigma} = 3$ curve from fig. 12 resulting in $r_e = 65$ km. On this day 129 strokes were detected, causing nearly 700 counts!

More of these rough analyses have been made; they all lead to r_e-values between 60 and 100 km for this type of storms. The unknown value of X imposes a serious restriction on the accuracy of these estimates.

4.10 Discussion

Some methods for estimating the effective range have been indicated. The application depends on the occurrence of suitable storms. Better data can be expected if these methods are used on more storms in the next years. For more accurate determinations however an independent locating and measuring system for atmospherics is necessary.

A large difference (about 10-70 km) in r_e has been found for warm-air respectively cold-air thunderstorms. The division between the groups is about -5 °C for the 700 mbar temperature, but it is yet unknown if there is a gradual transition of r_e or a sudden change. At this stage it should be mentioned that on a few occasions during the winter frontal storms did occur inland, which seemed to have a larger flash-rate and a lower r_e than the coastal storms discussed before (e.g. 1974 Dec. 10).

Due to their low lightning frequency (sections 6 and 10.3) and their large r_e the cold-air thunderstorms contribute very little to the yearly lightning flash-density. Future efforts to determine r_e should therefore concentrate on the more active summer storms.

We illustrate this with an example. If the average yearly total count (11 stations 1974-1976) is divided over the two T_{700}-groups and if we use the above-mentioned r_e-values for the respective groups, then

$$n = \frac{N_1}{\pi r_{e_1}^2} + \frac{N_2}{\pi r_{e_2}^2} = \frac{558}{\pi \cdot 10^2} + \frac{232}{\pi \cdot 70^2} = 1.78 + 0.15 = 1.93$$

strokes per square kilometre per year, or about 70,000 over the area of the Netherlands. With a 20% accuracy for r_e the true value of n will be between 1.3 and 2.7. This result is in accordance with other estimates at comparable geographic latitude (Golde, 1973).

The above figure of n considerably exceeds estimates based on reported lightning damage (e.g. Bleeker, 1936).

5. COMPARISON OF COUNTER RESULTS WITH THUNDER STATISTICS

5.1 Observations of thunder

Although lightning stroke counters operate on criteria quite different from the classic "thunder heard" observations, it might be of interest to compare both observing systems. Among the questions to be answered is whether the counters could replace the observers.

Thunder observations are primarily used in synoptic messages. Apart from their short-term application such observations are collected by the Climatology Department of the KNMI:

a. for climatological statistics;
b. to provide information on the possible occurrence on a certain date in the past of lightning or thunderstorm-related damage. Most of these questions come from insurance-companies.

Observations are collected from: synoptic stations (about 20 with hourly reports) and other stations (about 250, most of them with a rain-gauge). The network of volunteer observers was recently dismantled. The results of that network have been published in the series "Onweders...." (KNMI, 1880 etc.).

Apart from the internationally accepted practice to collect thunderstorm reports per station, the KNMI also used the method to combine the results of observers within 37 x 45 km rectangles laid in a grid over the country. This has been done to correct for missing observers etc.: in general to avoid that thunderstorms would remain unnoticed.

In the next paragraphs the data collected with the counters in the years 1974 through 1976 are compared with:

a. thunder reports from observers at the same location (5.2 and 5.3). During these years at 11 counter-stations synoptic observations were made;
b. thunder reports from the area surrounding the counter (5.6).

It should be kept in mind that this comparison between two imperfect systems is not suitable to judge the qualities of the lightning stroke counter as a thunderstorm detector.

5.2 General remarks

For a number of reasons there is no one-to-one relationship between a flash-counter registration and a thunder observation. The observer may not notice the phenomenon or mistakenly classify a different sound as thunder. The counter will - on the other hand - frequently operate on flashes from well outside the audibility range. Finally, the counter was designed with the purpose n o t to register intracloud or intercloud lightning.

Especially with low flashing rate a number of strokes may not be heard. A continuous watch in the open is impossible at most synoptic stations. So weak thunder can easily be missed. From all these arguments a rather poor correlation between instrument and observer may be expected, especially when considering hourly reports.

Thunderstorms are relatively rare phenomena: in the Netherlands, at any station, thunder is heard on less than 10% of the days. Therefore the usual techniques to quantify correlation fail. Under such circumstances two types of criteria can be given to check the coincidence between both observing systems:

a. for the estimation of statistics a criterion is to be preferred with a balance between the number of counted/not heard and heard/not counted situations;
b. for warning purposes a more conservative criterion would be better, provided that many false alarms be acceptable.

The network collects 10-min. totals. The obvious criterion will therefore be the count of at least a certain number of pulses during a specified period of time. That period can be chosen to start with a registration, but in this report only fixed hourly intervals (between the clock-hours) and fixed 24-hour periods (starting at 0000 GMT) are used.

5.3 Representation of days with thunder heard

If we consider all material of the three years for 11 stations, the number of thunderstorm days is almost equal to the number of days with at least 5 strokes counted ($N_d \geqslant 5$). The degree of success of this criterion is illustrated in fig. 23 for each station and for both the cold and warm half of the year.

A counter used with this criterion overestimates the occurrence of thunder at most of the coastal stations during the cold season. Compared to the other stations, thunder is apparently more easily heard at the central office at De Bilt. Perhaps this can be explained by the extra information about weak thunder that attentive colleagues pass to the observer.

The average result of the $N_d \geqslant 5$ criterion is that out of 23.9 thunder-days (average station per year) 6.1 were not detected, but that, for compensation, on 6.9 no-thunder-days the count reached 5 or more (Table 4).

Table 4 Thunder-day criteria for each season.

11 stations 1974 - 1976	Average number of days per year with: thunder	$N_d \geqslant 5$	both
Oct. - Mar.	2.6	4.4	1.4
Apr. - Sep.	21.3	20.3	16.4
Year	23.9	24.7	17.8 (75%)

Table 5 Thunder-day criteria for warm resp. cold airmass.

11 stations 1974 - 1976	Average number of days per year with: thunder	$N_d \geqslant 7$ if $T_{700} < -5$ $N_d \geqslant 3$ if $T_{700} \geqslant -5$	both
$T_{700} < -5^{\circ}C$	8.5	8.8	5.4
$T_{700} \geqslant -5^{\circ}C$	15.4	16.0	13.4
Year	23.9	24.8	18.8 (79%)

5.4 Separate criteria for warm resp. cold airmass

In the winter months separately the criterion $N_d \geqslant 5$ is very inaccurate: nearly half of the thunder-days is not recognized and many false alarms occur (Table 4). An improvement could be the use of $N_d \geqslant 4$ during the warm months and $N_d \geqslant 7$ for the rest of the year.

It seems preferable, however, to stratify the results with respect to the 700 mbar air temperature as was done in the previous sections. In fig. 24 the relative number of days is given that either the counter-criterion (full lines) or the observer (broken lines) did not reveal a thunderstorm-day. To improve the presentation T_{700} classes of 6 °C have been chosen, but a more detailed analysis shows indeed that a rather large jump of the broken line occurs at temperatures of about -6 °C. A separation in two groups seems therefore appropriate.

In the cold class there are evidently many counts on strokes outside the audibility range. If the criteria for the warm resp. cold class are taken as $N_d \geqslant 3$ resp. 7, only 21% of the thunder-days are not correctly identified (Table 5). For the low temperature group the full and broken lines in fig. 24 intersect at a much higher percentage than for the warm thunderstorm-days. For the latter group separately the criterion works more efficient: only 13% incorrect.

A different presentation of the degree of success of identifying thunderstorm-days with counters is given in fig. 25. In the class around $T_{700} = 5$ °C thunder is heard on almost any day the counter is triggered: $N_d \geqslant 1$ would then be the optimum choice.

Part of the difference between the curves in fig. 25 can be explained by the infrequent occurrence of low totals on warm days. This is illustrated in fig. 26: the cumulative frequency distribution of N_d for two T_{700}-classes.

Attention should also be given to the interdependence of the data, e.g. to the large contribution from a small number of summer days with widespread thunder and large counts at most of the 11 stations.

5.5 Comparison with hourly reports

Due to e.g. timing errors the correlation between hourly reports is expected to be weaker than with daily totals. It may be of interest to know the number of counts in a (fixed) hour that corresponds to the occurrence of thunder in that hourly interval.

Information on hourly counts N_h has already been presented in 3.8 and more will follow in section 6. Part of the data used for fig. 10 are summarized in Table 6.

Table 6 Hourly thunder reports compared with the counter.

De Bilt (+) 1973	Number of hourly intervals with thunder	$N_h \geqslant 2$	both
$T_{700} < -5$	38	40	21
$T_{700} \geqslant -5$	41	36	32
All	79	76	53 (67%)

As mentioned in 5.3 De Bilt is not a very suitable station. Table 7 contains data from two geographically contrasting stations (Fig. 11). De Kooij is a coastal station situated in flat country, whereas Zuid-Limburg is a more continental station in a hilly region. For both $N_h \geqslant 3$ is the best criterion ($N_h \geqslant 1$ is the trivial choice for an alarm-criterion). In contrast to the daily totals the use of separate criteria for warm and cold situations would be no advantage.

Table 7 Hourly thunder observations (1974-1976).

		Number of hours per year with thunder	$N_h \geqslant 3$	$N_h \geqslant 2$	$N_h \geqslant 1$
De Kooij	Oct. - Mar.	19	18	30	62
	Apr. - Sep.	38	38	52	99
	Year	57	56	82	161
Zuid-Limburg	Oct. - Mar.	3	2	5	20
	Apr. - Sep.	50	47	65	118
	Year	53	49	70	138

5.6 Comparison with reports from the surrounding area

In 5.1 the practice at the KNMI of combining stations has been mentioned. By doing this a better correlation with the counter registrations can be expected. The grid of counter stations however does not correspond to the rectangle-grid used by the Climatology-Department.

Therefore this comparison has been carried out by using so-called Thiessen-polygons: each station is compared with that part of the country for which that station is the nearest counter.

Table 8 Combined thunder reports.

average of 18 stations 1974	Number of days per year with thunder	$N_d \geqslant 2$	both
Oct. - Mar.	12.1	15.7	9.0
Apr. - Sep.	33.3 ± 4.9	33.0 ± 3.8	27.4
Year	45.4	48.7	36.4 (80%)

The results of table 8 can be compared with the 11 stations of table 4. For 1974 alone, the coincidence was 77%, while for the corresponding 11 stations in the above table it was 81%. Although the gain is marginal, the counter will also "keep watch" over a larger area if $N_d \geqslant 2$ is taken.

For the summer months the standard deviation for the series of 18 separate stations (resp. areas) is given in table 8. The counters suggest that thunderstorms are more uniformly distributed over the country!

Finally, attention is given to a record kept by the Climatology-Department of the number of days that anywhere in the Netherlands thunder was heard. Of course the area is rather arbitrary. The average of the 3 years (1974-1976) was 100 days per year. On 98 days per year the count at at least one of the stations exceeded 2. On 86 days (87%) both phenomena occurred.

6. APPLICATIONS OF THE NETWORK (examples)

6.1 Two case-studies

Some characteristics of autumn and winter thunderstorms have received attention in the preceding sections. The network can also provide interesting information in situations with e.g. severe thunderstorms. The counter results are a supplement to rainfall maps, regular observations, radar pictures and reports on damaging hail or wind.

An example may illustrate this.

- 1974, Aug. 16-17 (Fig. 27)

During this night a cold front travelled from west to east over the country after a few days of warm summer weather: a rather typical event in Western Europe. Conditions for the development of severe storms were favourable: e.g. a strong southwesterly jetstream. Hail damage was especially severe in a greenhouse area in the southeast of the country near Venlo (fig. 27c). The surface damage has been described elsewhere (Hattinga Verschure, 1976). After crossing the German border the hail continued (Emmrich, 1976). The composite picture of the flash rate shows that the thunderstorms passed in two series. Before midnight prefrontal airmass showers developed in the eastern part of the country. Conditions in the coastal region became less favourable for convection because of a seabreeze that invaded during the afternoon. After midnight a second line of storms intruded from the south. These storms travelled with the actual cold front and were restricted to the area southeast of the line from Bergen-op-Zoom to Hoogeveen. The extension of this line to the southwest remains inland all through Brittany, so the squall-line that moved with the upper southwesterly wind could profit over a long distance from warm low-level air. This is a common feature during cold-front intrusions in summer.

A mesoscale characteristic of such squall-lines is the concentration of hail- and wind-damage at the right-front edge of the progressing line. Near Venlo the hail measured up to 8 cm diameter. More northerly cells like the one that passed at 0245

near Volkel with up to 8 counts per minute were electrically more active (compare with Heibloem). This cell passed north of Twenthe at about 0350. The hail north of Twenthe fell from a cell ahead of the main front. A preceding cell will profit likewise from an undisturbed low-level inflow as a cell at the right front edge.

- 1975, May 7 (Fig. 28)

  These storms also caused wind damage and large hail but travelled more slowly than those of the first example. Most storms were arranged along a west-east line that slowly moved to the northwest under the influence of a low pressure centre in the southwest. On the composite flash-rate record fig. 28a, a few strokes can be seen that probably triggered different counters, e.g. just after 1440 and after 2030. Most of the flashes did only trigger the nearest counter, as would correspond with an r_e of about 10 km. In the flash-rate registrations the passing of different cells can be recognized.

  The correlation between the total number of flashes and the close passage of storms is quite good (fig. 28c). The low counts of De Kooij and Lelystad are in agreement with their distances of more than 30 km from the major storm tracks. The thunder areas of figures 27c and 28c do correspond very well with the counter registrations. The same applies to most summer situations.

- Case-studies can be useful for thunderstorm forecasting and for investigating atmospheric electric phenomena. Among the possibilities for research are e.g. the correlation between flash-rate and synoptic situation, rain- and hail-production, radar data etc.

6.2 Preliminary climatological results

The network has been installed to collect two types of data: information on the occurrence of lightning and also on the intensity of thunderstorms. Many numerical values concerning the first item has been presented with the examples of section 5. In fig. 26 the

cumulative frequency distribution of daily totals has been shown. During the first three years of the network the record for N_d was reached at Raalte on July 8 1975 with 907. On the same day the nearby counter at Hoogeveen had 873. The count of that one day was for these stations 64% resp. 52% of the total for 1975. Most of these strokes occurred within two hours!

Although this may be an extreme example, the large contribution of a few heavy nearby thunderstorms to the yearly total causes an appreciable spread in the yearly totals. Fig. 29 presents the distribution of seasonal and yearly totals for each of the three years. Apparently this period is too short to draw final conclusions, especially while the low-activity year 1976 is included. The yearly counts of neighbouring stations seem to correlate well, especially in the southwest-northeast direction, which is parallel to the tracks of most of the major storms.

The effective range of the counter has a suitable value to inform us about regional differences, but due to the erratic appearance of the heaviest storms a longer period of observation will be necessary to draw conclusions.

Meanwhile, care should be taken to maintain the comparability of the stations. The only prominent feature of fig. 29 is the influence of the autumn coastal storms discussed before. It may be noted that this type of storms was rare during 1975.

6.3 Regional, diurnal and seasonal differences in lightning frequency

In the tables 9 and 10 a detailed comparison between two stations in opposite corners of the territory of the Netherlands is presented. The listing of table 9 shows some "statistical noise", but it is clear that most flashes at the continental station Zuid-Limburg occur during the afternoon and early evening in the summer months. At the coastal station De Kooij a second type of showers appears after the sea has been warmed. This type of thunderstorms has a slight maximum during the night hours. Such storms may occur until January.

Table 9 Total count in three years for each hour and each month (1974-1976).

DE KOOIJ

	03			06			09			12			15			18			21 gmt		
J				1						1	1					1	1	1	10	3	4	1		
F							1			1														
M																			1					
A							1			1					1						1			
M								1	1	9	3		5	1	7			1	6	1	3		12	18
J	1		2	2	4	10	3	1	11	3	5	6	11	26	16	16	2	12	31	5	1	1	4	25
J	3	2		5	1		3	5	6	7	27	31	144	13	14	1	2		25			2		1
A	1	3	58	20	1	3	3	5	131	220	31	40	33	3	6	2	14	2		3	10	7	1	
S	39	25	16	50	38	5	6	5	4	8	11	17	6	7	24	24	26	22	6	20	19	34	60	99
O	5	2	10	23	7	5	4	3	19	2	3	8	2	3	5	2	3	1	5	2	1	16	6	3
N	10	6	18	24	4	5	3	10	8	3	4				1	6	2	10	22	23	12	9	17	31
D	10	11	3	9	12	19	6	7	11	5	6	3	8	5	3		2	2	2	2	4	4	3	3

ZUID-LIMBURG (AERODROME)

	03			06			09			12			15			18			21 gmt		
J				1										1		1				1	1
F							1		1		1			1	1		1	2			
M										1	1		2		2	4	1	1		1	2	2		
A									1		2	4	1								1			
M				31	16			1	4	17	28	34	98	19	46	12	11	4	2	10	1			
J	10	1							1	3	69	158	88	78	62	50	42	54	39	5	6	101	12	1
J	3	11	6	56	4	7		1	4	1	5	13	11	32	54	53	72	35	38	150	18	15	15	10
A	19	1	14	7	1	1	4	1		1	14	4	13	14	35	80	106	35	14	11	33	9	11	6
S	44	1	2	1	1	5	7	10		2	2		3	21	4	9	19	15	5	7	3		110	52
O			1	1			1					2	1	4	6	3	4	2						
N				1					1		1						8	1	3	1				
D			1	2		1	2						1				4	6	12					1

Table 10 Number of hours with at least 3 counted. Total for three years (1974-1976) (i.e. about 0.9 times the percentage probability).

DE KOOIJ

	03			06			09			12			15			18			21 gmt		
J																2					
F																					
M																					
A																					
M	1									1	1		1		1				1		
J					1	1	1		1		1	1	2	1	3	2		1	2		
J				1				1	1	1	4	4	3	1	2						
A		1	1	1				1	2	2	3	2	1		1		1			1	
S	4	3	2	2	2		1			1	2	2		1	5	3	3	3	1	3	2
O	1		1	2	1	1		1	1			1									
N	2	1	1	1		1	1	2	1		1					1		2	2	1	1
D	1	1		2	2	1	1	1	1	1	1		2	1							1

	21 gmt		
J			
F			
M			
A			
M		2	1
J			1
J			
A	1		
S	4	3	6
O	1	1	
N	2	2	2
D	1		

ZUID-LIMBURG (AERODROME)

	03			06			09			12			15			18			21 gmt		
J																					
F																					
M																					
A																					
M				1	1					3	3	3	4	3	3	2	1			1	
J	1										1	3	5	5	1	4	3	2	2	1	1
J	1	2	1	1		2					1	1	3	1	7	4	3	3	2	1	3
A	1		1	1			1				1		1	3	1	5	3	2	1	1	1
S	1					1	1	2						3		2	2	1		1	
O															1						
N																	1		1		
D																	1	1	1		

	21 gmt		
J			
F			
M			
A			
M			
J	2	2	
J	2	1	1
A	2	2	1
S	1	1	
O			
N			
D			

In table 10 thunderstorm hours are selected with the criterion of 5.5. In this way the differences are even more clearly visible than in the table with total counts. The figures can be regarded as an estimate of the percentage probability of thunder in the respective hours.

These stations do not so much show differences in the number of thunder-days or in the number of flashes as in the daily and seasonal distribution. High flash frequencies are more likely at continental stations. In 1974 37 of the 10-minute totals of Zuid-Limburg were 10 or more against only 5 at De Kooij. Apart from a direct maritime influence also the upper-air temperature gradient will play a role: during thunderstorm situations T_{700} above De Kooij will be a few degrees lower than above Zuid-Limburg. High flash rates (>1 per min.) almost exclusively occur for $T_{700} > -5\ ^{o}C$. More information is given in Appendix 10.3

From these arguments it is clear that in the quantitative interpretation of counter results (e.g. 4.10) such systematic differences will have to be taken into account.

7. SOME CONCLUSIONS

7.1 Compared to the human observer the described counter has the advantage to be objective, to operate continuously and to be essentially insensitive to horizontal discharges.

7.2 The main disadvantage is the variable maximum reporting distance, due to the non-uniformity of the properties of lightning strokes. This disadvantage also applies to thunder-heard reports. Techniques have been suggested to estimate the "effective range" for various categories of storms. It is recommended that calibrations of the counter are continued. It is also suggested that comparisons as mentioned in section 3.4 be carried out.

7.3 Criteria have been found to use the counter for warning, reporting and collecting statistical thunder data. Days with 7 resp. 3 counts can be considered thunder-days in cold resp. warm airmasses. Hours with at least 3 counts correspond to nearby thunderstorms in all seasons.

7.4 The measurements show large differences in amplitude, sign and frequency of the atmospherics with changing upper-air temperature. This is important for the interpretation of the counter-registrations but might also be of interest to atmospheric physics, because it involves the location of charging and discharging mechanisms with respect to the 0 ^{o}C level. Autumn and winter lightning strokes should receive more attention. They seem to carry large currents and represent therefore a considerable risk. It would be of interest to explain the combination of low flash rate and violent strokes during the cold season.

8. ACKNOWLEDGEMENTS

Thanks are due to the director-in-chief of the Royal Netherlands Meteorological Institute (KNMI) for his permission to undertake this study. The instalment and operation of this network naturally involved the help of many people, in- and outside the KNMI. The author is especially indebted to Mr. F.P.M. Bekkers for the circuit design, to Dr. J.P. de Jongh for the numerical integration of equation (22), to Mr. H.J.A. Vesseur for valuable advice, to Mr. C.A. Engeldal and Mr. W.P.A.G. Ottevanger who shared part of the responsibility for the network and to Maj. J.H. Boer of the Royal Netherlands Air Force for helpful discussions on lightning counters.

9. REFERENCES

R.A. Barham, 1965. A transistorised lightning-flash counter. IEE Electronics Letters 1, 173.

W. Bleeker, 1936. Verdeling der blikseminslagen over Nederland. Hemel en Dampkring 34, 428.

J.H. Boer 1967. A verification of the accuracy of short-range lightning counters. Weather 22, 321-330.

R.E. Bogner, J,F. Conners, 1967. Shielding factors for electrostatic aerials. Proc. IEE 114, 1425-1427.

C.E.R. Bruce, R.H. Golde, 1941. The lightning discharge. J. Inst. Elec. Eng. 88 Part 2, 487-520.

J.A. Chalmers, 1967. Atmospheric Electricity. 2nd ed., Oxford, 515 pp.

D.L. Croom, 1964. The frequency spectra and attenuation of atmospherics in the range 1-15 kc/s. J. of Atm. Terr. Phys. 26, 1015-1046.

P. Emmrich, 1976. Bemerkungen zum Hagelfront vom 17. und 18. August 1974. Meteor. Rdsch. 29, 54-61.

G. Frühauf, H.G. Amberg, W. Wurster, 1966. Wirkungsweise und Reichweite von Blitzzählern. Beihefte der ETZ, Heft 6 (VDE-Verlag).

R.H. Golde, 1973. Lightning protection. Edward Arnold, London.

P.P. Hattinga Verschure, 1976. Het noodweer rond Venlo op 17 augustus 1974. Zenit 3, 135-138.

F. Horner, 1960. The design and use of instruments for counting local lightning flashes.
Proc. IEE 107, B, 321-330.

F. Horner, 1967. Analysis of data from lightning-flash counters.
Proc. IEE 114, 916-923.

H. Israël, 1961. Atmosphärische Elektrizität II,
Leipzig, 502 pp.

T. Kikushi, T. Araki, 1972. Distortion of VLF radio wave field by vertical metal poles.
Contr. Geoph. Inst., Kyoto Univ. 12, 1-5.

KNMI 1880-1965. Onweders, Optische Verschijnselen enz. in Nederland.
Publ. nr. 81, Pt. 1 - 82.

M.J. Large, E.T. Pierce, 1955. The fine structure of natural point-discharge currents.
Q. J. of the Roy. Met. Soc. 81, 92-95.

J.A. Leise, W.L. Taylor, 1977. A transmission line model with general velocities for lightning.
J. Geoph. Res. 82. 391-396.

D.K. Mc Lain, M.A. Uman, 1971. Exact expression and moment approximation for the electric field intensity of the lightning return stroke.
J. Geoph. Res. 76, 2101-2105.

D.J. Malan, 1963. Physics of lightning,
London, 176 pp.

R.B. Morrison, 1953. The variation with distance in the range 0-100 km of atmospheric wave-forms.
Philosophical Mag. 44, 7th Ser., 980-986.

D. Müller-Hillebrand, 1963. Lightning counters, I, II.
Arkiv för Geofysik 4, 247-269, 271-292.

F. Ollendorf, 1932. Potentialfelder der Elektrotehcnik, Berlin.

W.P.A.G. Ottevanger, 1970. Bliksemtellers in Nederland.
Hemel en Dampkring 68, 304-308.

E.T. Pierce, 1956. The influence of individual variations in the field changes due to lightning discharges upon the design and performance of lightning-flash counters.
Arch. Met. Geoph, Biokl. A, 9, 78-86.

S.A. Prentice, D. Mackerras, 1969. Recording range of a lightning-flash counter.
Proc. IEE 116, 294-302.

L.H. Ruhnke, 1971. Determining distance to lightning strokes from a single station.
NOAA Techn. Rep. ERL 195/APCL 16.

B.F.J. Schonland, D.J. Malan, H. Collens, 1935. Progressive lightning Pt.2.
Proc. Roy. Soc. (London) A 152, 595-626.

A.W. Sullivan, I.D. Wells, 1957. A lightning stroke counter.
Bull.Am.Met.Soc., 38, 291-294.

T. Takeuti, M. Nakano, M. Nagatani, H. Nakeda, 1973.
On lightning discharges in winter thunderstorms.
J. of the Met. Soc. of Japan 51, 494-496.

J.A. Tiller, M.A. Uman, Y.T. Lin, R.D. Brantley, 1976.
Electric field statistics for close lightning return strokes near Gainesville, Florida.
J. Geoph. Res. 81, 4430-4434.

M.A. Uman, 1969. Lightning. New York, 264 pp.

M.A. Uman, D.K. McLain, R.J. Fisher, E.Ph. Krider, 1973.
Electric Field intensity of the lightning return stroke.
J. Geoph. Res. 78, 3523-3529.

M.A. Uman, C.E. Swanberg, J.A. Tiller, Y.T. Lin, E.P. Krider, 1976.
Effects of 200 km propagation on Florida lightning return stroke electric fields.
Radio Science 11, 985-990.

W.M.O. 1959. An instrument for counting local lightning flashes.
W.M.O. bull. 8, 19-23.

10.1 APPENDIX A: CAPACITY OF AN ELEVATED VERTICAL ROD

First the potential is derived caused by a charge Q equally distributed along a thin line (fig. 30). The contribution to the potential at the point (x,z) by each line element $d\zeta$ with charge $\frac{Q}{2l} d\zeta$ is

$$d\varphi = \frac{Q}{4\pi\varepsilon_o} \frac{1}{2l} \frac{d\zeta}{\sqrt{x^2+(\zeta-z)^2}}$$

Integrating this from $\zeta = -l$ to $+l$ results in the potential

$$\varphi = \frac{Q}{4\pi\varepsilon_o} \frac{1}{2l} \ln \frac{l-z+\sqrt{x^2+(l-z)^2}}{-l-z+\sqrt{x^2+(-l-z)^2}} \qquad (23)$$

The equipotential planes can be shown to be rotational-symmetrical ellipsoids with focal points in $z = +l$ and $z = -l$ and with semi-axes (a,a,c)

$$\varphi = \frac{Q}{4\pi\varepsilon_o} \frac{1}{2l} \ln \frac{c+l}{c-l} \qquad (24)$$

Therefore this is also the potential of a charged conducting stretched ellipsoid with long axis 2c and numerical excentricity $\frac{l}{c}$. It is of interest to consider the far-field potential in cartesian coordinates.

For $x << |z-l|$ and $x << |z+l|$ (23) reduces to:

$$\varphi = \frac{Q}{4\pi\varepsilon_o} \frac{1}{2l} \ln \frac{z+l}{z-l} \qquad (25)$$

This treatment of the potential around a conducting rod can be found in textbooks (Ollendorf, 1932, p. 93).

The presence of a conducting plane perpendicular to the z-axis of $z = -h$ can be accounted for by adding to (24) the potential due to a mirror-ellipsoid with charge $-Q$ centred at $z = -2h$. The resulting potential with respect to the conducting plane at the surface of the ellipsoid becomes

$$\varphi = \frac{Q}{4\pi\varepsilon_o} \frac{1}{2l} \left(\ln \frac{c+l}{c-l} - \ln \frac{2h+l}{2h-l} \right) \tag{26}$$

For a thin rod ($a = \sqrt{c^2 - l^2} < c$) the capacity to earth is given by

$$C_A = \frac{Q}{\varphi} = \frac{2\pi\varepsilon_o \cdot 2l}{\ln \frac{2l}{a} - \frac{1}{2} \ln \frac{2h+l}{2h-l}} \tag{27}$$

The last term in the denominator can be neglected if $l \ll h$.

10.2 APPENDIX B: CRITERIA FOR THE DISTURBANCE OF THE ELECTROSTATIC FIELD NEAR THE EARTH'S SURFACE CAUSED BY OBSTACLES

The aerial of a lightning counter has to detect an undisturbed change of the electric field. We suppose that any distortion of the electrostatic field results in a proportional error of the field change.

The electric field will be disturbed by any dielectric or conducting structure rising above ground level. For simplicity we describe such an obstacle as the upper half of a conducting stretched rotational ellipsoid, placed in a vertical position. The semi-axes are a,a,c. The restriction to conducting obstacles is more or less justified, because buildings, trees etc. will generally be wet during situations with nearby thunderstorms.

The polarization of a stretched ellipsoid in a field with strength E (V/m) parallel to the long axis is treated by Ollendorf (1932, p. 314). The solution for the potential as it is modified by a conducting ellipsoid can be written

$$\varphi(z) = -E\left(z - c\cdot\frac{v}{l}\cdot\frac{\frac{1}{2}\frac{u}{l}\ln\frac{u+l}{u-l} - 1}{\frac{1}{2}\frac{c}{l}\ln\frac{c+l}{c-l} - 1}\right) \qquad (28)$$

The variables u and v are so-called elliptic coordinates:

$$x = \frac{\sqrt{u^2-l^2}\cdot\sqrt{v^2-l^2}}{l} \quad \text{and} \quad z = \frac{uv}{l} \qquad \text{(fig. 31).}$$

For reasons of symmetry we have z = 0 as an equipotential plane with the same potential as the ellipsoid-surface. The field-strength in the z = 0 plane is found from

$$-\frac{\partial\varphi}{\partial z} = -\frac{\partial\varphi}{\partial v}\frac{\partial v}{\partial z} = \frac{\partial\varphi}{\partial v}\cdot\frac{l}{u}$$

because $\frac{\partial\varphi}{\partial u} = 0$ for z = 0. The field strength is therefore

$$-\frac{\partial\varphi}{\partial z} = E\left(1 - \frac{c}{u}\,\frac{\frac{1}{2}\frac{u}{l}\ln\frac{u+l}{u-l} - 1}{\frac{1}{2}\frac{c}{l}\ln\frac{c+l}{c-l} - 1}\right)$$

In the $z = 0$ plane we have $x = \sqrt{u^2 - \iota^2}$. Using the eccentricity $e = \frac{\iota}{c} = \sqrt{1-(\frac{a}{c})^2}$ we arrive at

$$-\frac{\partial \varphi}{\partial z} = E\left[1 - \frac{1}{\sqrt{(\frac{x}{c})^2 - e^2}} \cdot \frac{\left\{\frac{\sqrt{(\frac{x}{c})^2+e^2}}{e^2} \ln\left(\frac{c}{x}\sqrt{(\frac{x}{c})^2+e^2}+e\right) - 1\right\}}{\left\{\frac{1}{e}\ln\frac{c}{x}(1+e) - 1\right\}}\right] \qquad (29)$$

In fig. 31 the relative disturbance of E has been plotted as a function of $\frac{x}{c}$ for some values of $\frac{a}{c}$. For convenience we have chosen the height of the obstacle as reference length.

For a spherical obstacle ($\frac{a}{c} = 1$) with radius c a much simpler derivation leads to

$$-\frac{\partial \varphi}{\partial z} = E\left\{1 - (\frac{x}{c})^{-3}\right\} \qquad (30)$$

These calculations can also be extended to structures with horizontal dimensions larger than twice the height. Such a structure is simplified here to a flat spherical ellipsoid with focal points at the cross-section in the plane $z = 0$ on the circle $x^2 + y^2 = \iota^2$. For this object we arrive in an analogous way at

$$-\frac{\partial \varphi}{\partial z} = E\left[1 - \frac{\arctan\left\{\left(\frac{x}{c}\cdot\frac{c}{a}\cdot\frac{1}{e}\right)^2 - 1\right\}^{-\frac{1}{2}} - \left\{\left(\frac{x}{c}\cdot\frac{c}{a}\cdot\frac{1}{e}\right)^2 - 1\right\}^{-\frac{1}{2}}}{\arctan\left(\frac{a}{c}e\right) - \frac{a}{c}e}\right] \qquad (31)$$

For the flat ellipsoid we use $e = \frac{\iota}{a} = \sqrt{1 - \left(\frac{c}{a}\right)^2}$
The two curves for large $\frac{a}{c}$ in fig. 31 illustrate this case.

From these results it can be concluded that the field is weakened by less than 1% at a distance greater than twice the height of a thin obstacle like a lamp-post. In other situations the errors can easily be estimated with fig. 31.

In addition it should be noted that the field-error declines with the third power of the distance, at least if the obstacle is not too close. For horizontally elongated obstacles like dikes, long buildings, rows of trees, the error falls off with the second

power of the distance. A few lines to illustrate errors near elliptical cylinders are also included in fig. 31. It may be helpful that a relatively small displacement of the aerial can sometimes lead to a large reduction of the error.

10.3 APPENDIX C: OBSERVED LIGHTNING FREQUENCY IN THE NETHERLANDS (1956-1965)

A remarkably complete set of published data is available on the occurrence of thunderstorms and related phenomena in the Netherlands "Onweders,...." (KNMI, 1880-1965). Among the editors was during the early years KNMI's first director-in-chief C.H.D. Buys Ballot. The publication was based on observations of a few hundred volunteer observers. This network was rather dense: the average distance was about 10 km.

Since 1956 tables have been included which combined thunderstorm observations and synoptic parameters. Among the entries were the 500 mbar temperature (estimated for the thunderstorm-environment) and the maximum repetition frequency of lightning reported on the relevant day.

To show the relation between flash frequency and airmass-temperature fig. 32 has been prepared, based on about 1000 thunder-days. The corresponding 700 mbar temperatures were estimated by applying a wet-adiabatic displacement. The 500 mbar temperature-classes correspond with the T_{700}-classes used in this report.

Lightning-stroke frequencies in summer and winter storms apparently can differ by a factor of nearly 100. Unfortunately, the data in fig. 32 refer to the maximum and not to the average flash rate. Also a large proportion of horizontal discharges will be included. Anyway it illustrates the behaviour of a well-developed storm under the prevailing conditions.

From fig. 32 no sudden change in flashing behaviour around $T_{700} = -5\ ^{o}C$ can be suspected.

The frequency of occurrence of a thunder-day (anywhere in the Netherlands) is between 26 and 30% for all 8 temperature classes

used in constructing this figure. The average probability is 28%. From this large amount of data there is no indication that the probability of the development of at least one thunderstorm in the country depends on the upper-air temperature. Evidently, other factors like e.g. stability are more relevant.

In the tables referred to, also the number of reported lightning strokes with damage are included. The number of earth strokes with reported damage is very small compared to all earth flashes. With the material available there is some indication that the fraction of observed flashes that cause damage, is decreasing for higher flash rates. This is partly connected with the higher percentage of horizontal flashes at higher temperatures: the well-known decrease of the proportion of horizontal flashes with increasing geographic latitude can also be interpreted with the upper-air temperature as parameter (partly determining the height of the charge centres). The large-amplitude sferics produced during autumn-thunderstorms do also indicate that currents in these strokes are rather large.

Statistics like those in fig. 32 can of course be collected with lightning-counter data in the future.

-o-o-o-

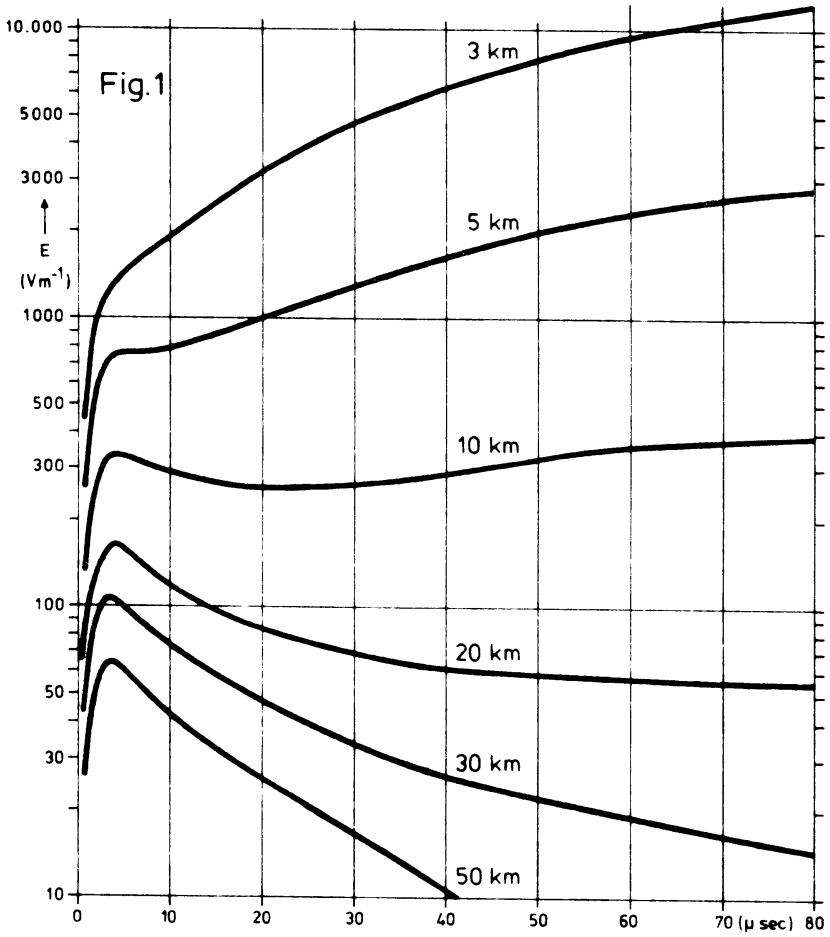

Fig. 1

Field change (as a function of time and distance) caused by an idealized stroke to earth.
(h_o=2400 m, i_o=22 kA, $\alpha=10^4$, $\beta=5.10^5$, $\gamma=3.10^4$).

Fig. 2

Frequency spectrum of the field change around the discharge specified for fig. 1.
Curve (a) is the frequency response-curve of the KNMI-counter in relative units.

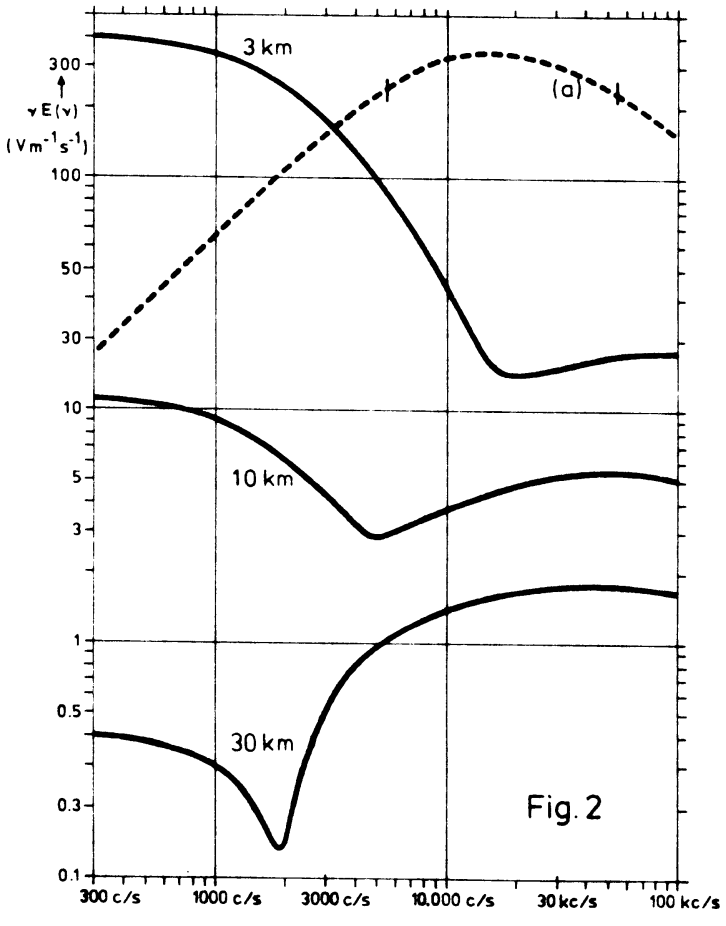

Fig. 3

Increase of potential within the first 50 μs at varying range from the stroke of fig. 1.

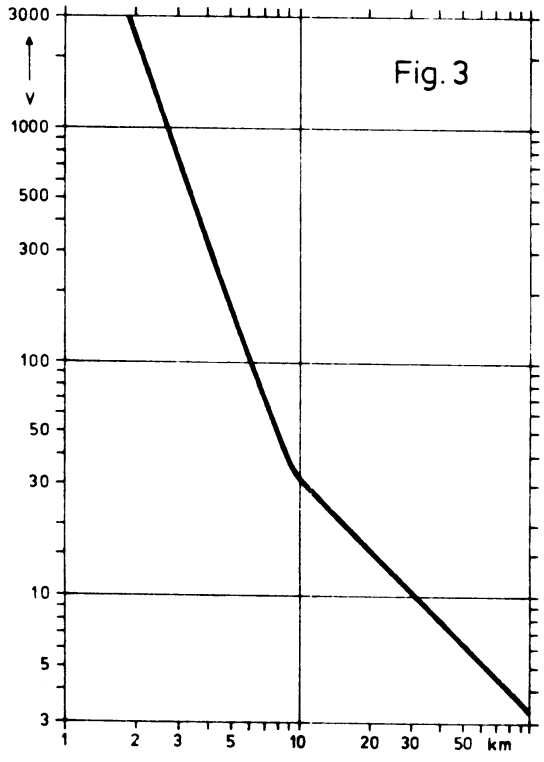

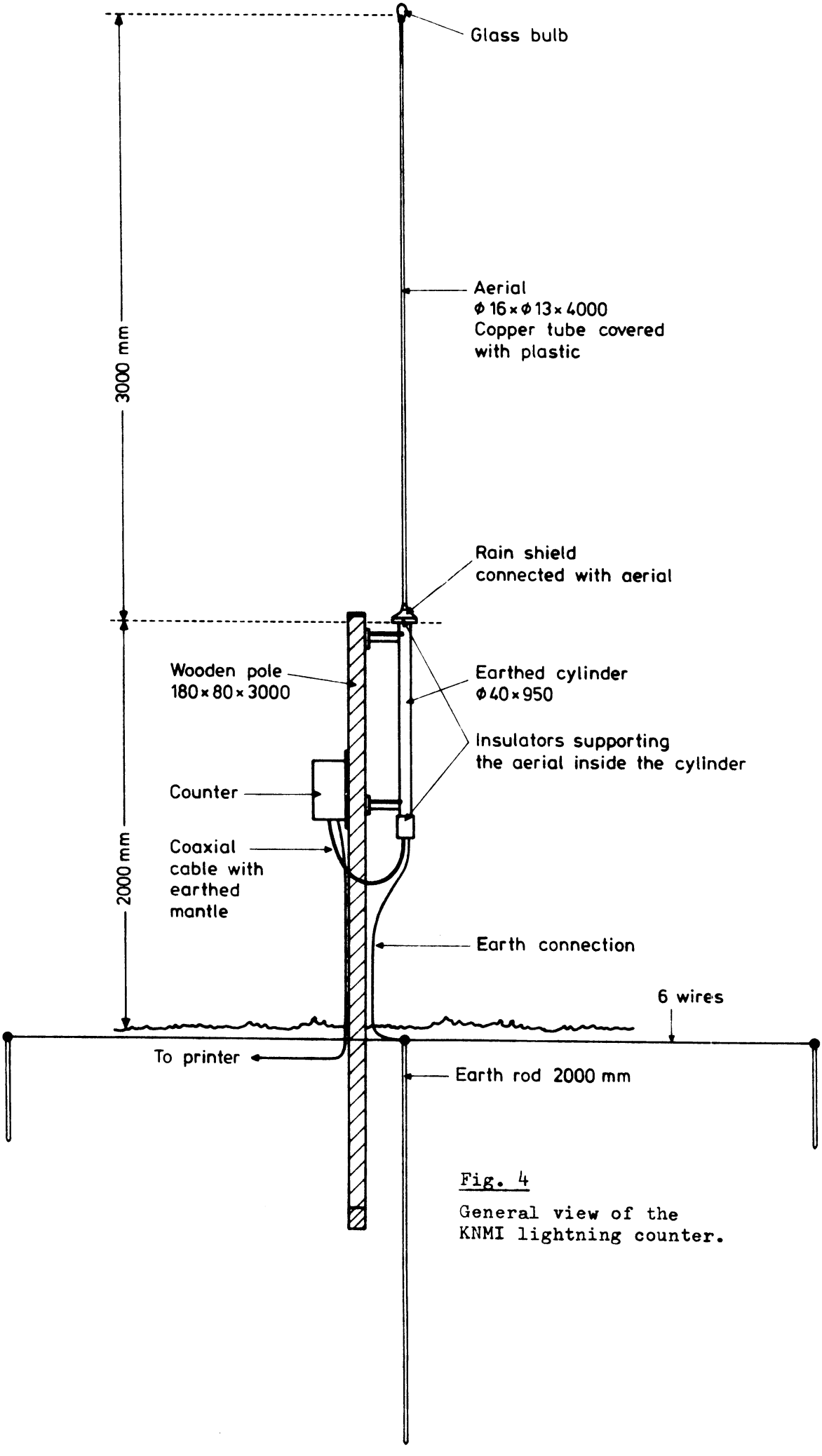

Fig. 4

General view of the
KNMI lightning counter.

K.N.M.I. LIGHTNING COUNTER

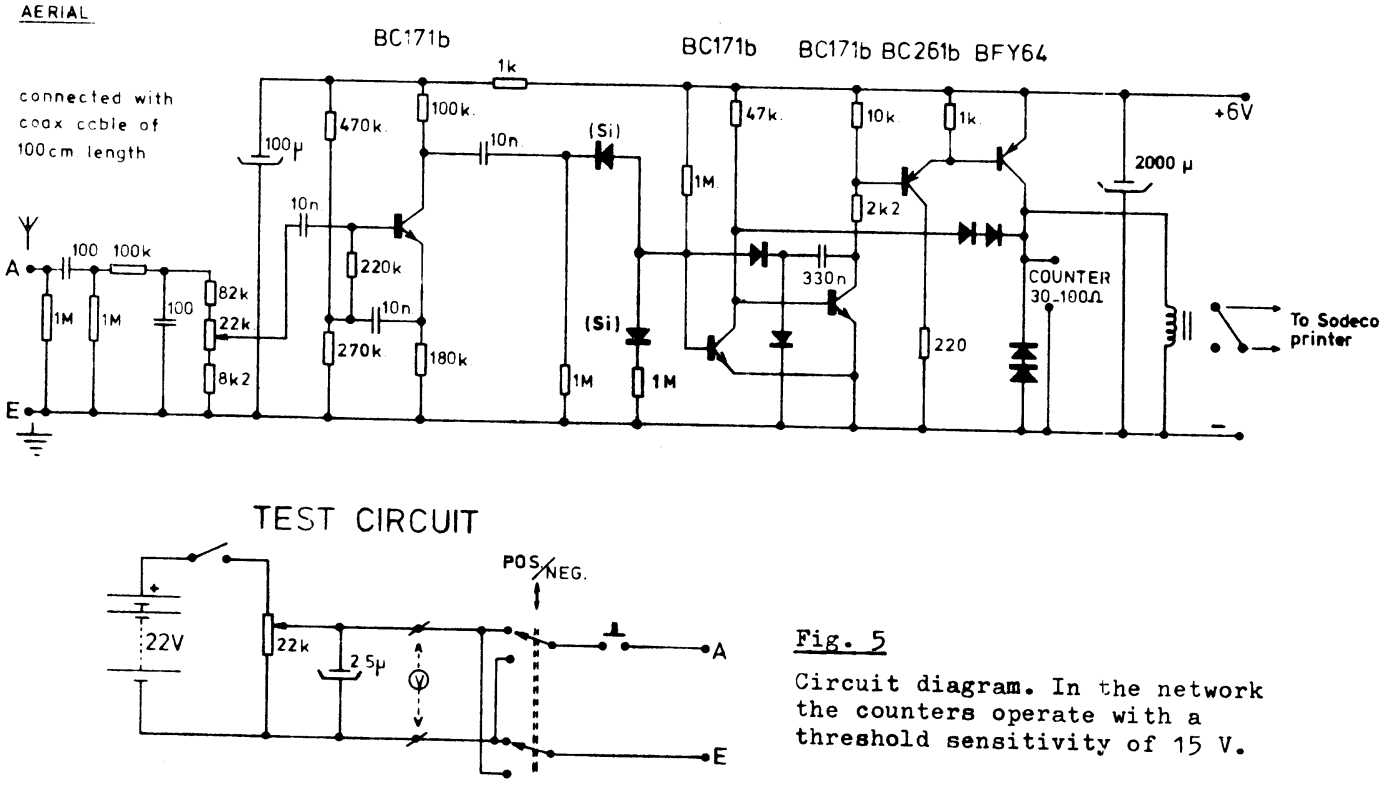

Fig. 5

Circuit diagram. In the network the counters operate with a threshold sensitivity of 15 V.

Fig. 6

To illustrate the potential acquired by the aerial after a field change. C_A is the capacity between aerial and earth.

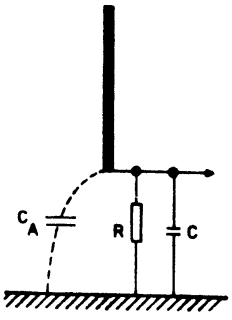

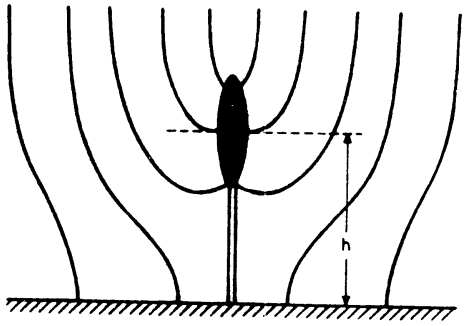

Fig. 7

Vertical field distorted by an earthed vertical rod (sketch).

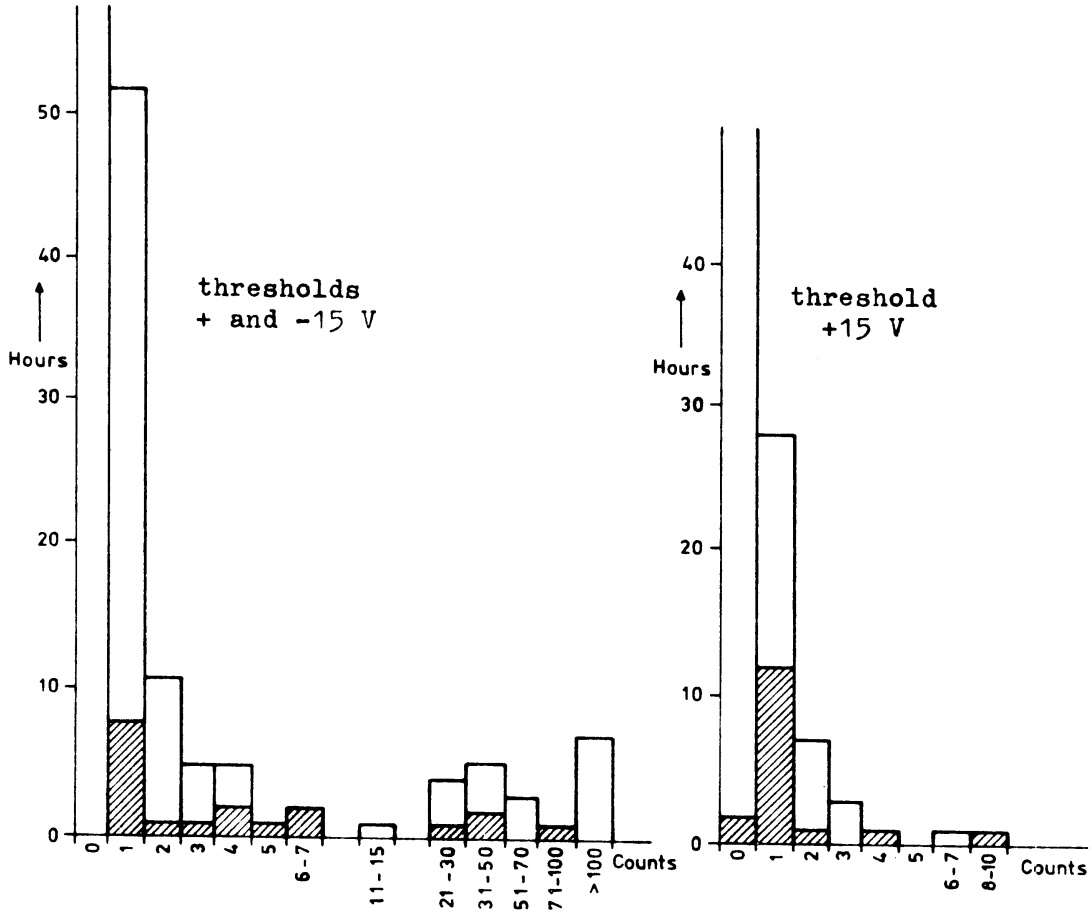

Fig. 8

Vlissingen, 1973 Nov. 25 - 1974 Apr. 25.
Number of hourly counts in the classes indicated along the abscissa.
Cases with thunder heard within about 20 km are hatched.

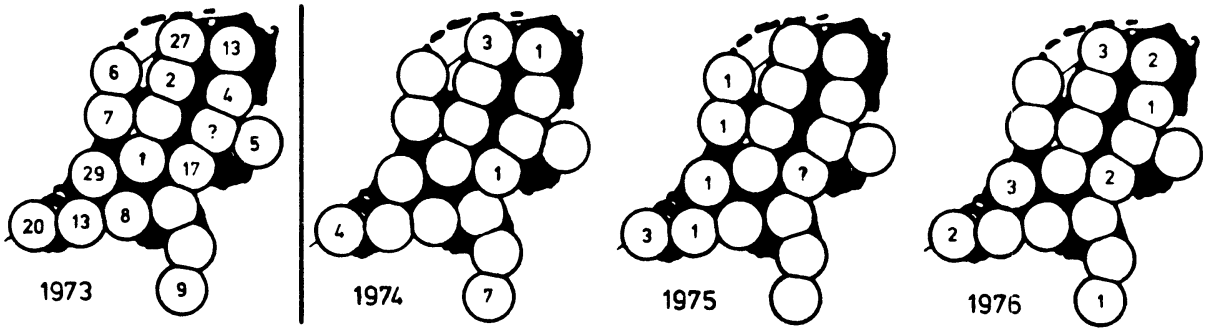

Fig. 9

Number of days per year when point discharge triggered the counter.
Before (1973) and after (1974 onwards) the exclusion of negative field-jumps.

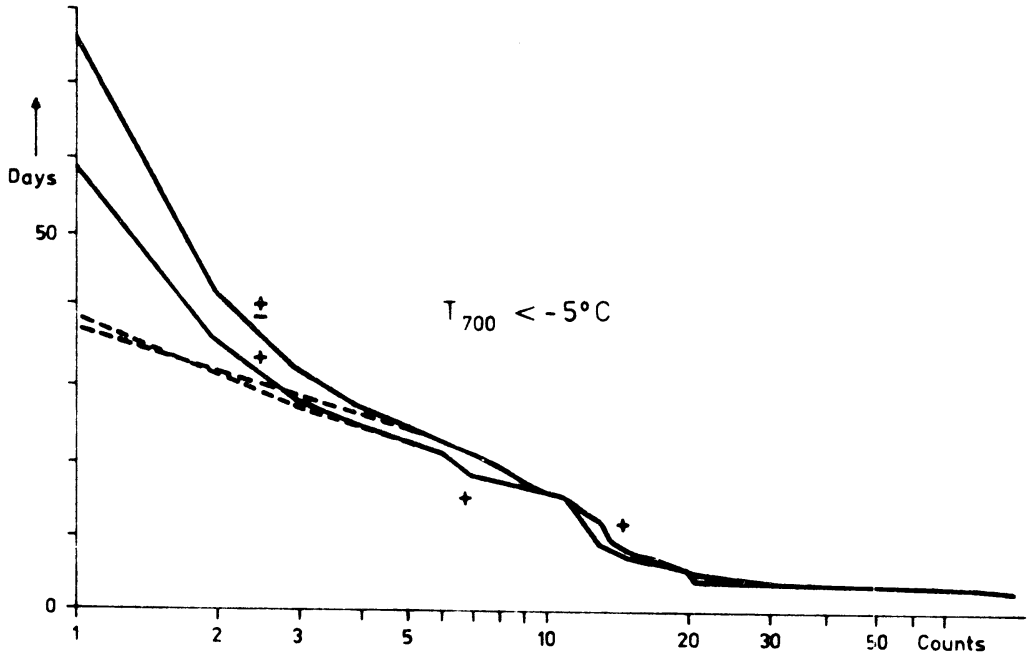

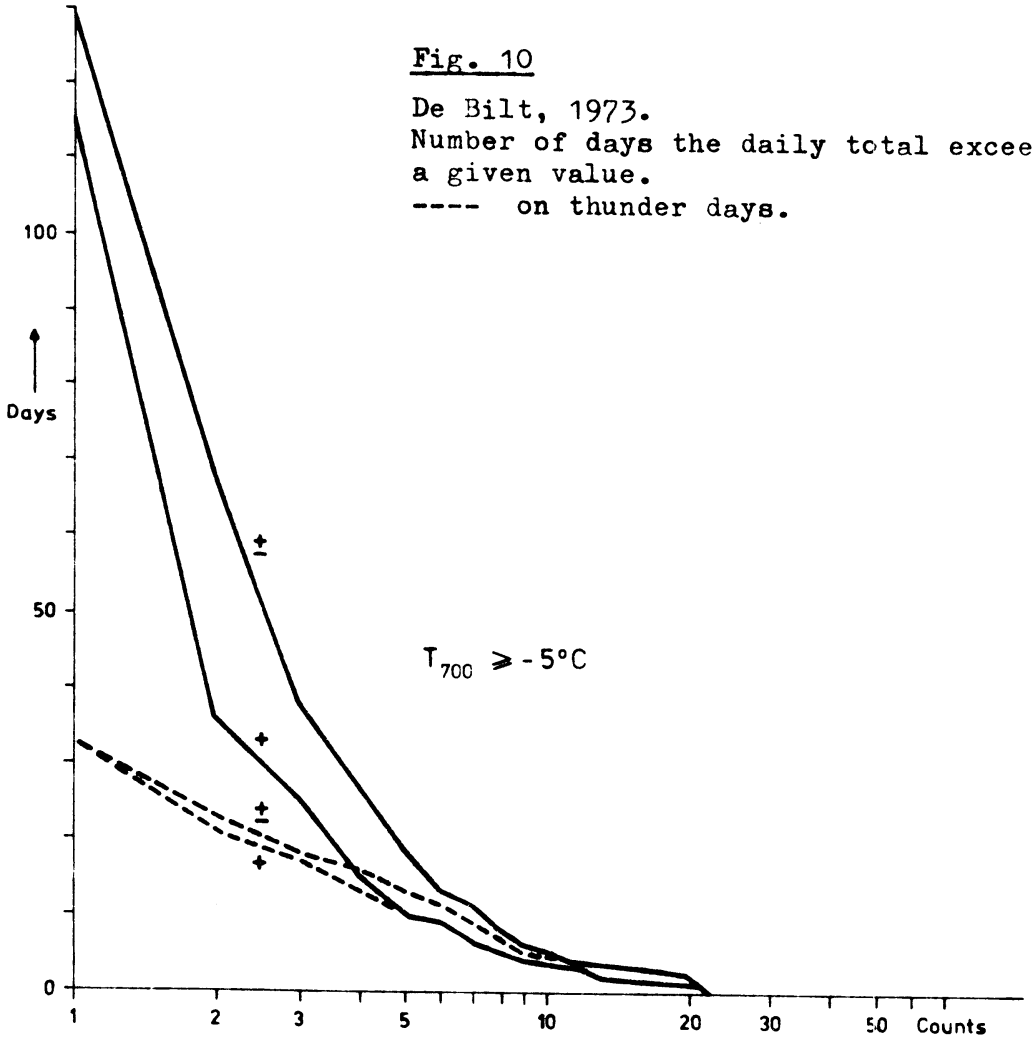

Fig. 10

De Bilt, 1973.
Number of days the daily total exceeded a given value.
---- on thunder days.

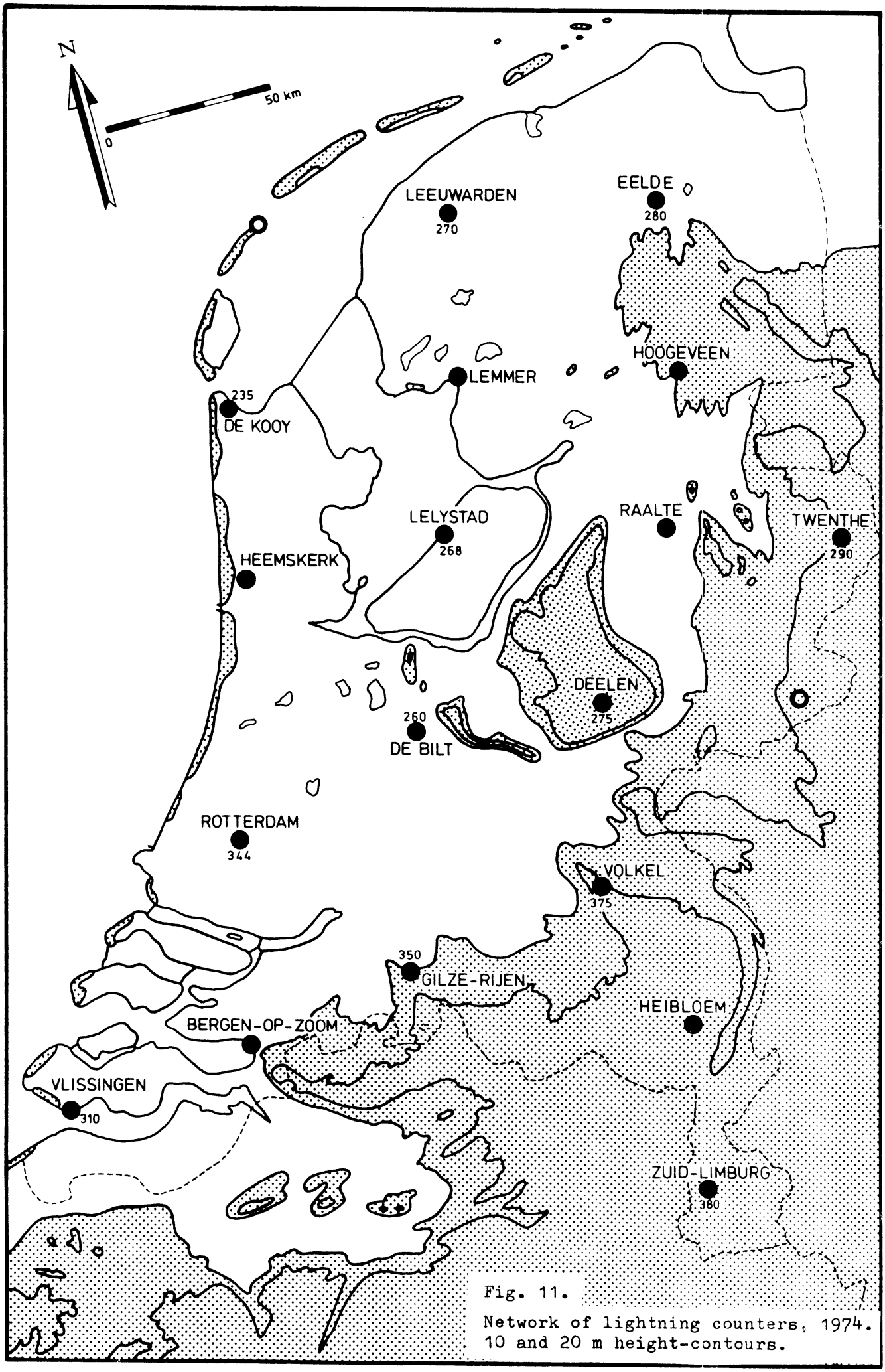

Fig. 11.
Network of lightning counters, 1974.
10 and 20 m height-contours.

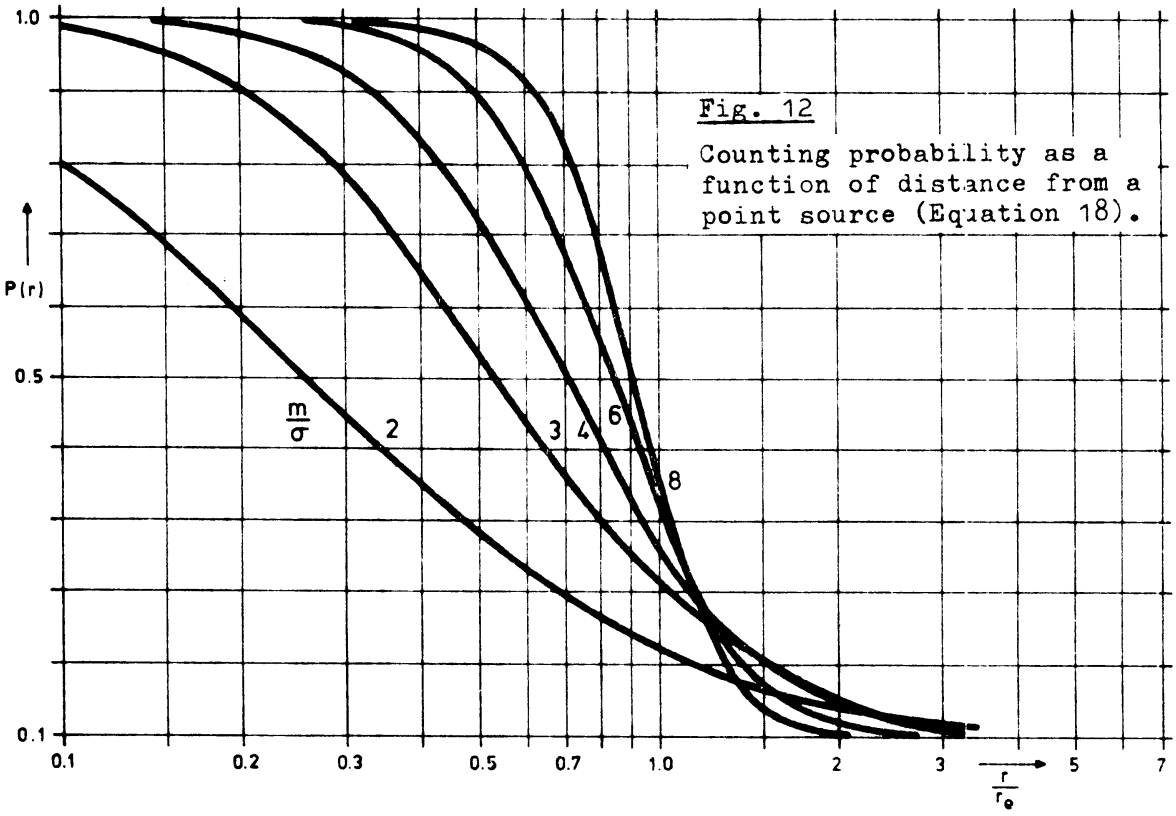

Fig. 12

Counting probability as a function of distance from a point source (Equation 18).

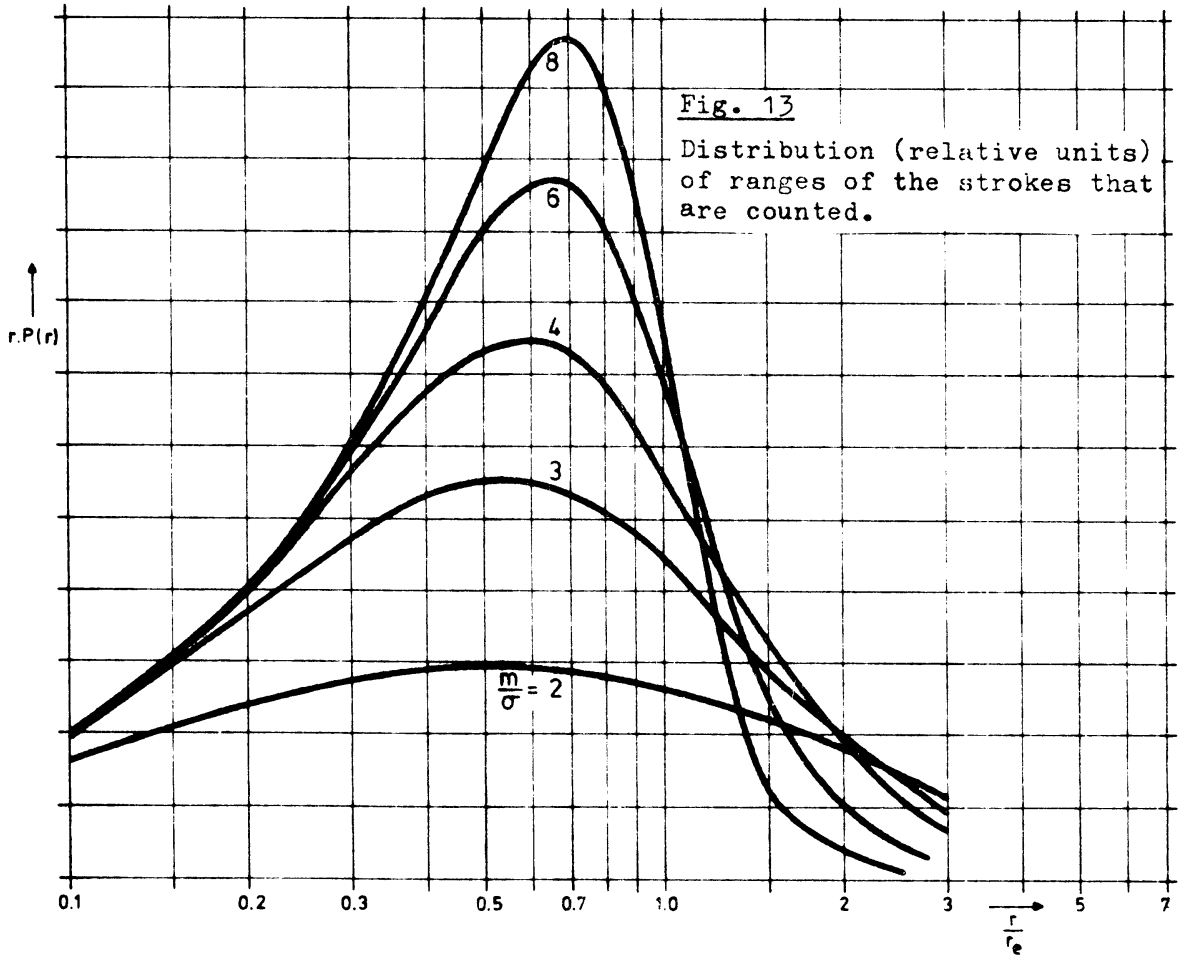

Fig. 13

Distribution (relative units) of ranges of the strokes that are counted.

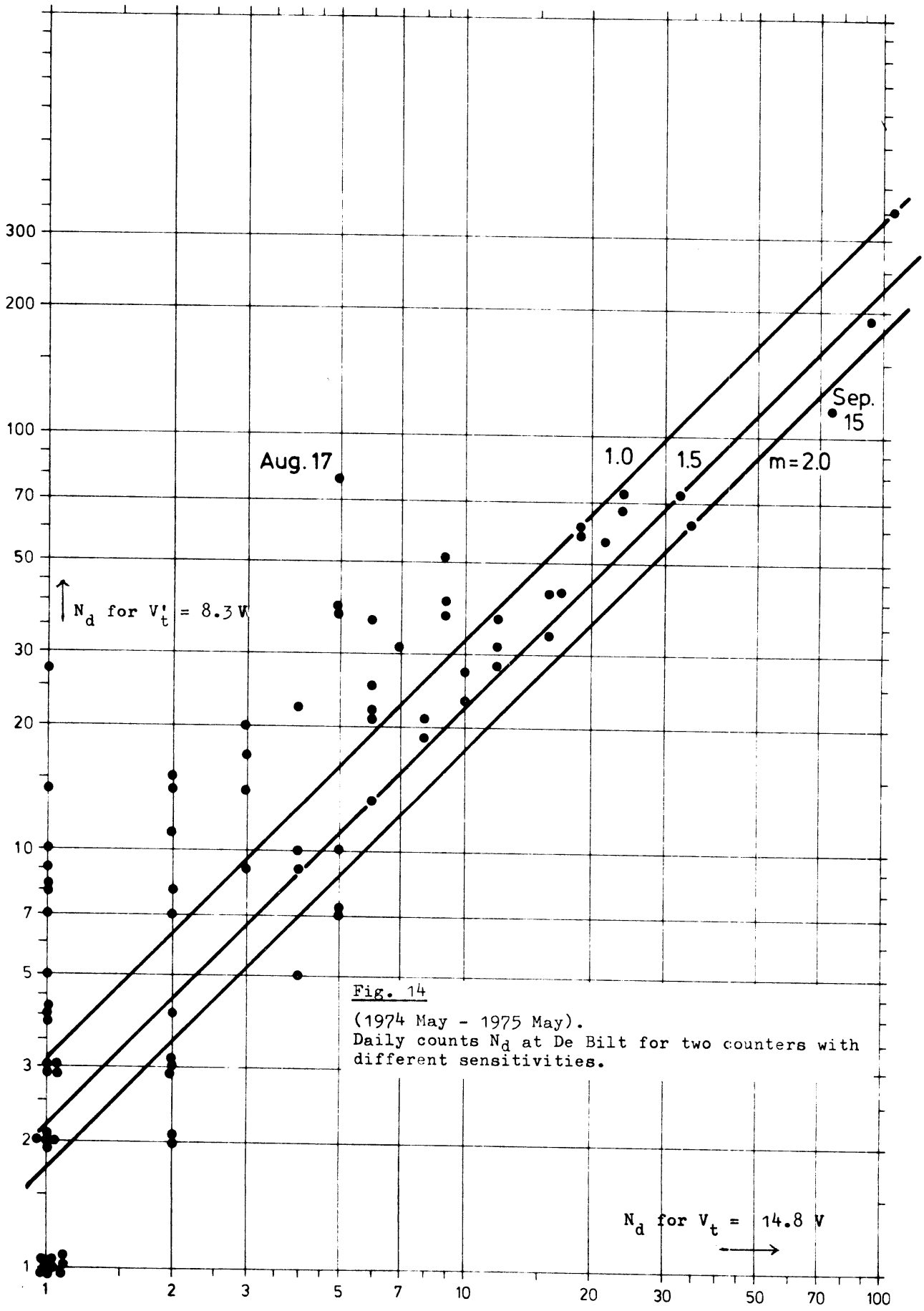

Fig. 14

(1974 May - 1975 May).
Daily counts N_d at De Bilt for two counters with different sensitivities.

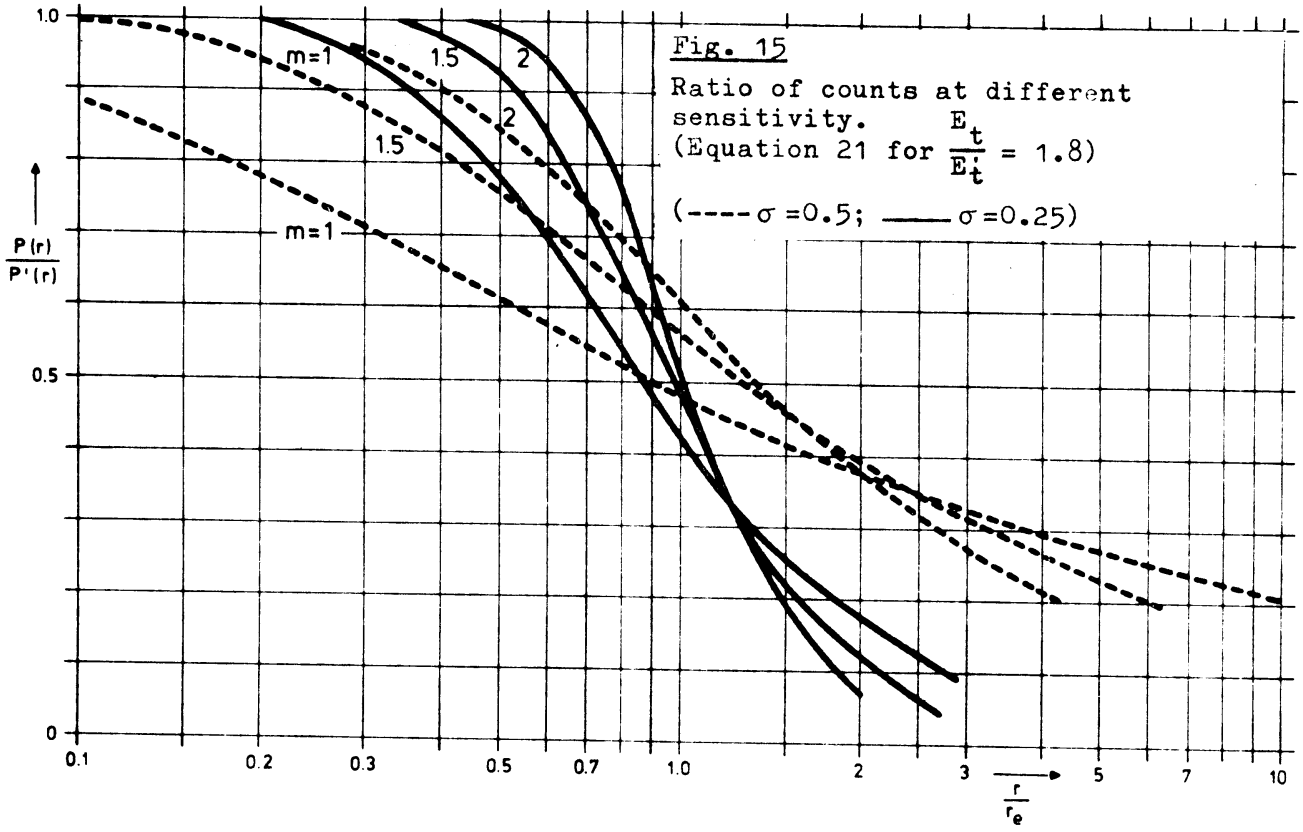

Fig. 15

Ratio of counts at different sensitivity. $\frac{E_t}{E_t'} = 1.8$)

(---- $\sigma = 0.5$; ——— $\sigma = 0.25$)

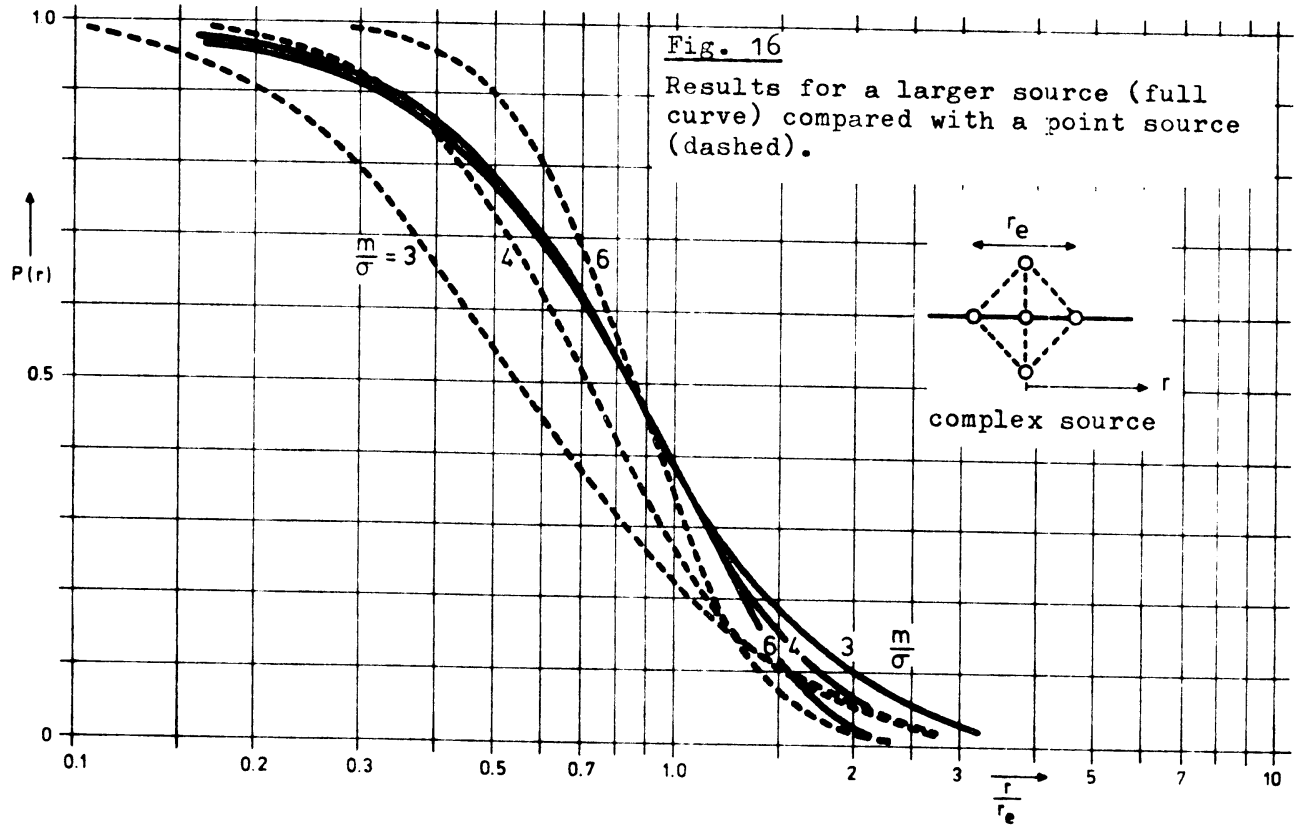

Fig. 16

Results for a larger source (full curve) compared with a point source (dashed).

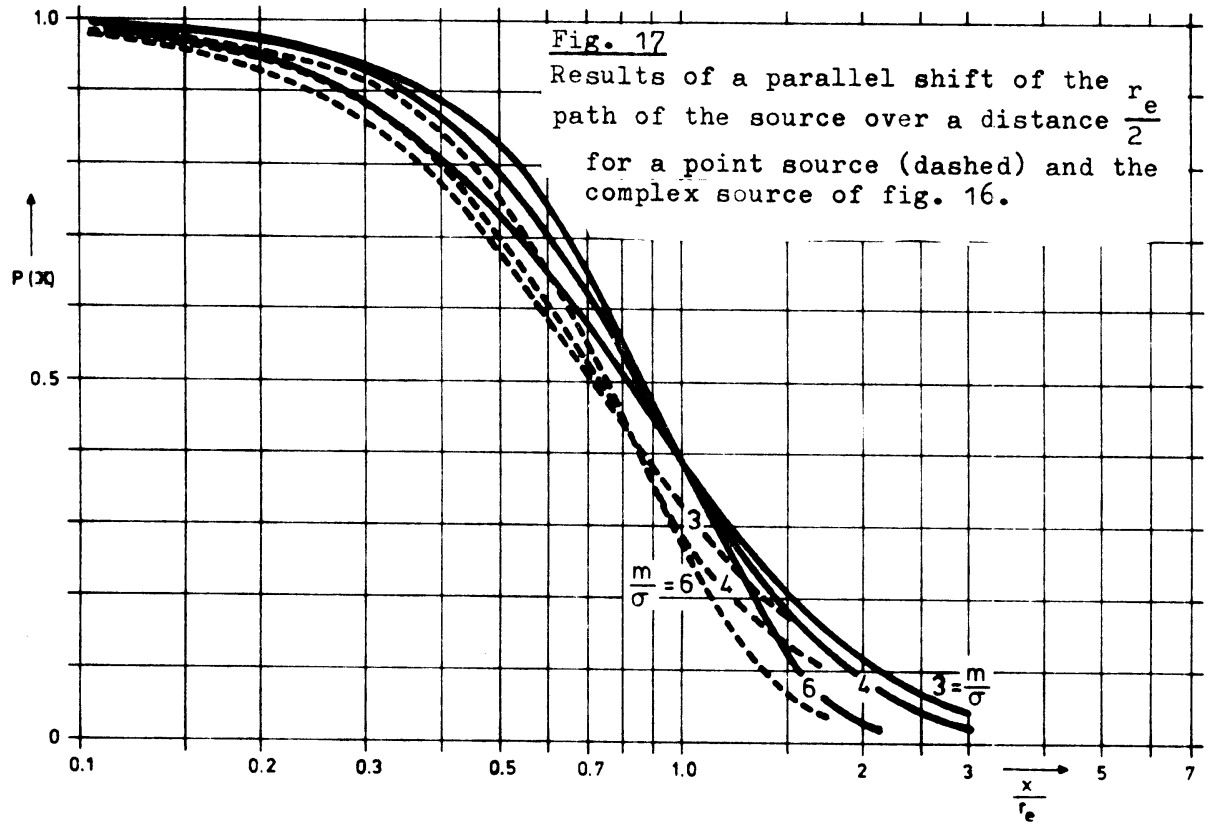

Fig. 17
Results of a parallel shift of the path of the source over a distance $\frac{r_e}{2}$ for a point source (dashed) and the complex source of fig. 16.

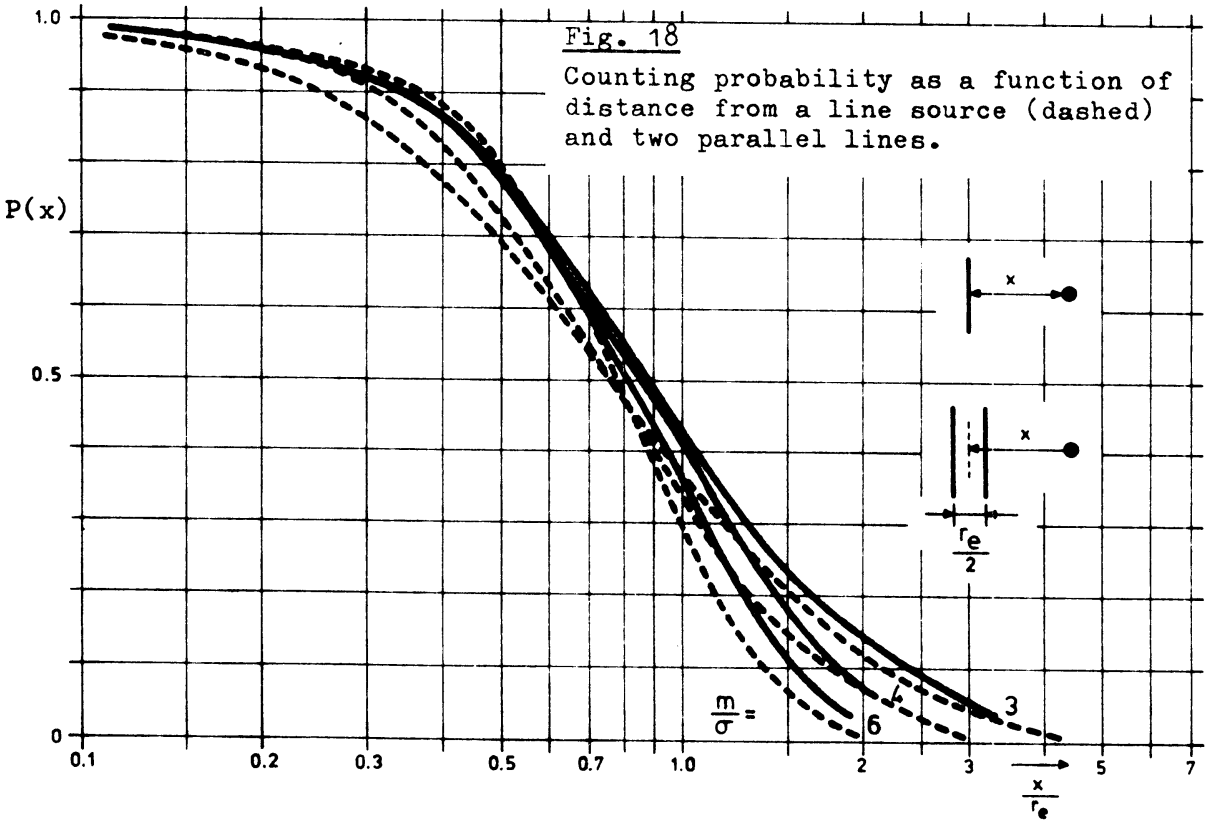

Fig. 18
Counting probability as a function of distance from a line source (dashed) and two parallel lines.

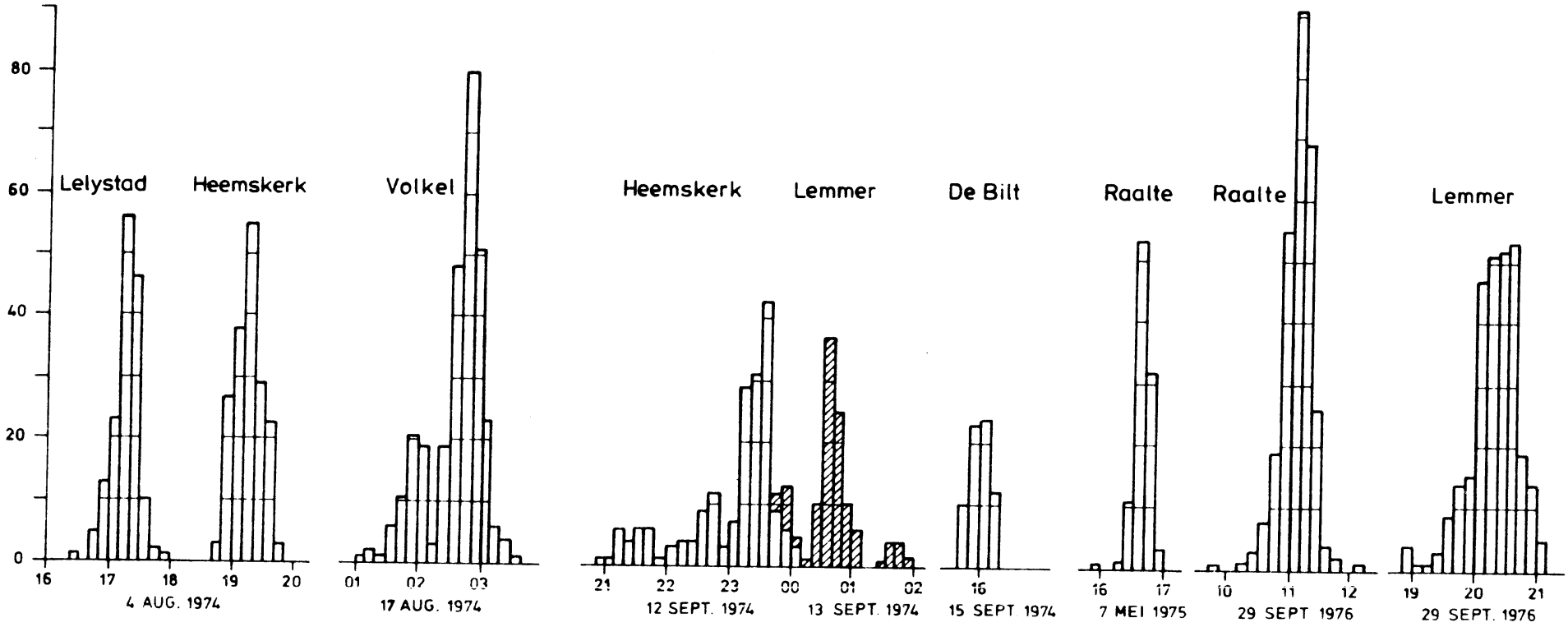

Fig. 19 10 min. counts for 9 selected storms.

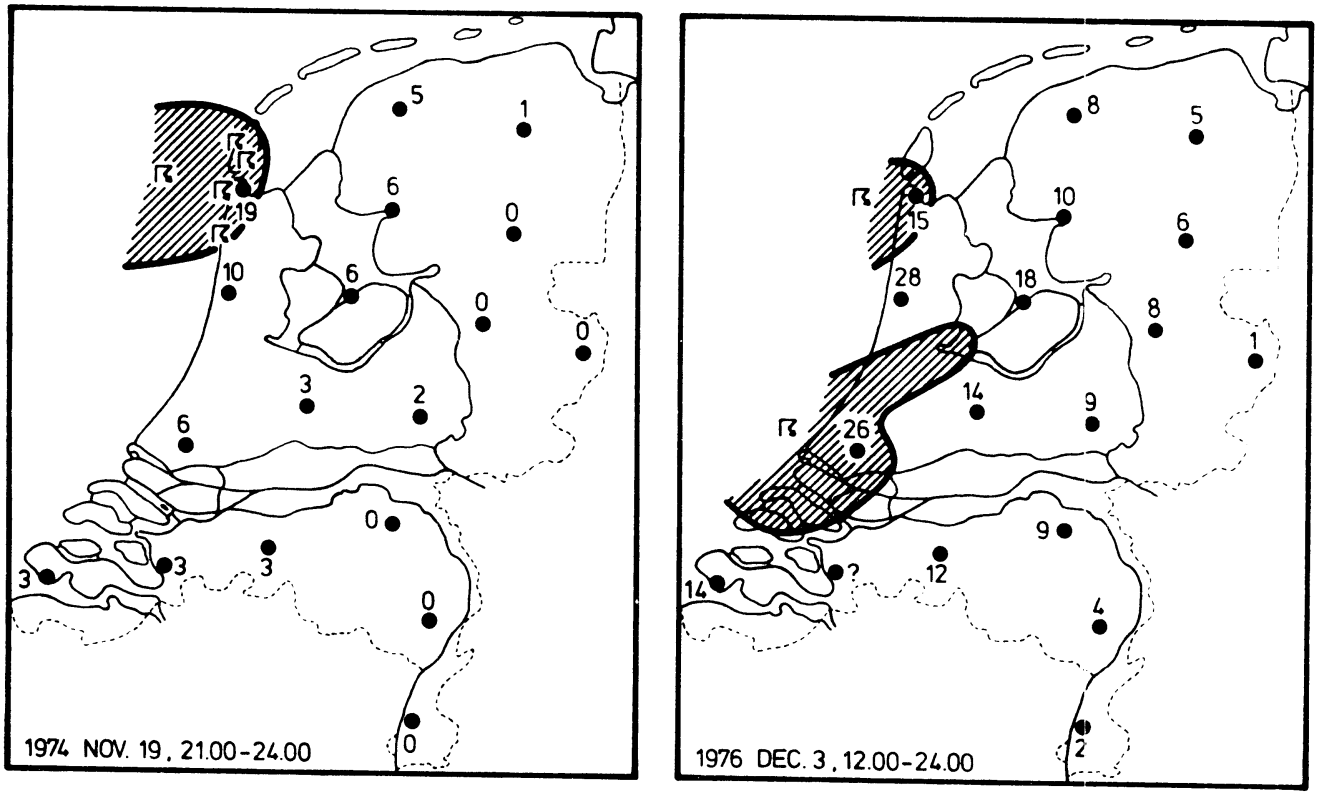

Fig. 20 and 21 Total counts in relation to areas with thunder heard.

Fig. 22 Distribution of triggering ranges for all flashes on two days.

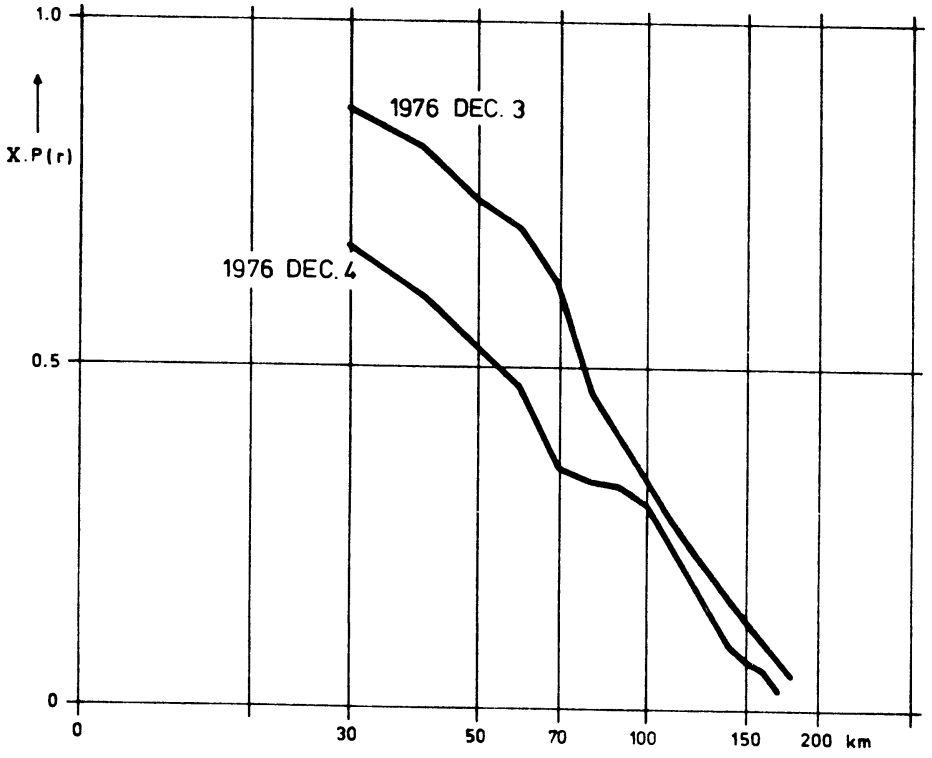

Fig. 23

Number of days in 3 years with:

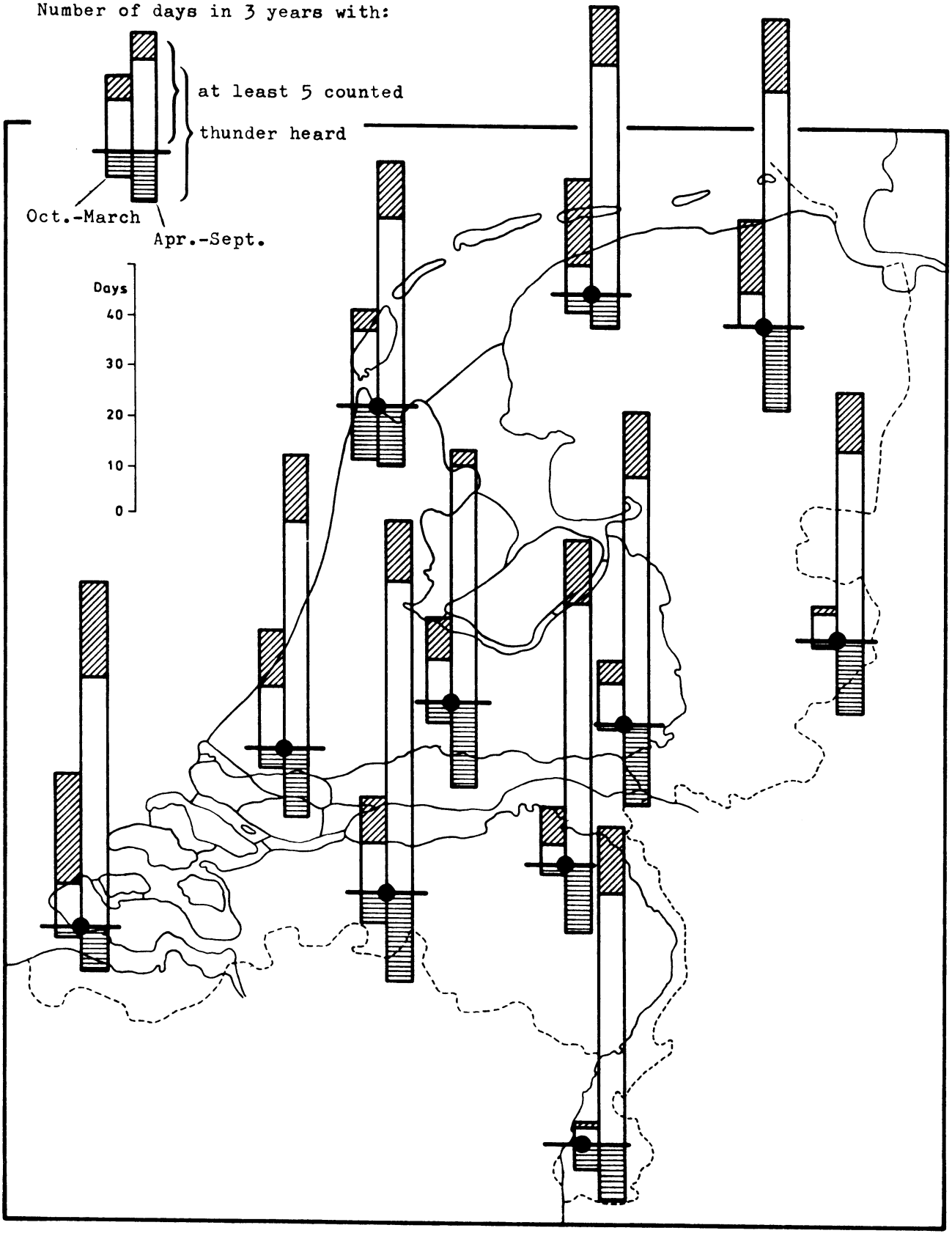

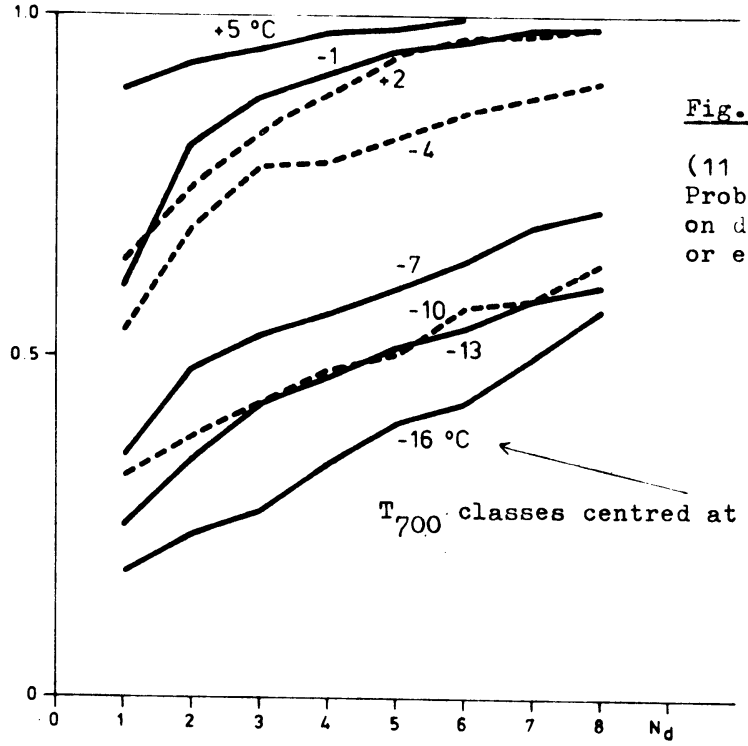

Fig. 25

(11 stations, 3 years). Probability of thunder on days with N_d reached or exceeded.

Fig. 24 (11 stations, 3 years).

---- Number of no-thunder days with N_d exceeded / Number of thunderstorm days

—— Fraction of thunderstorm days with N_d not reached.

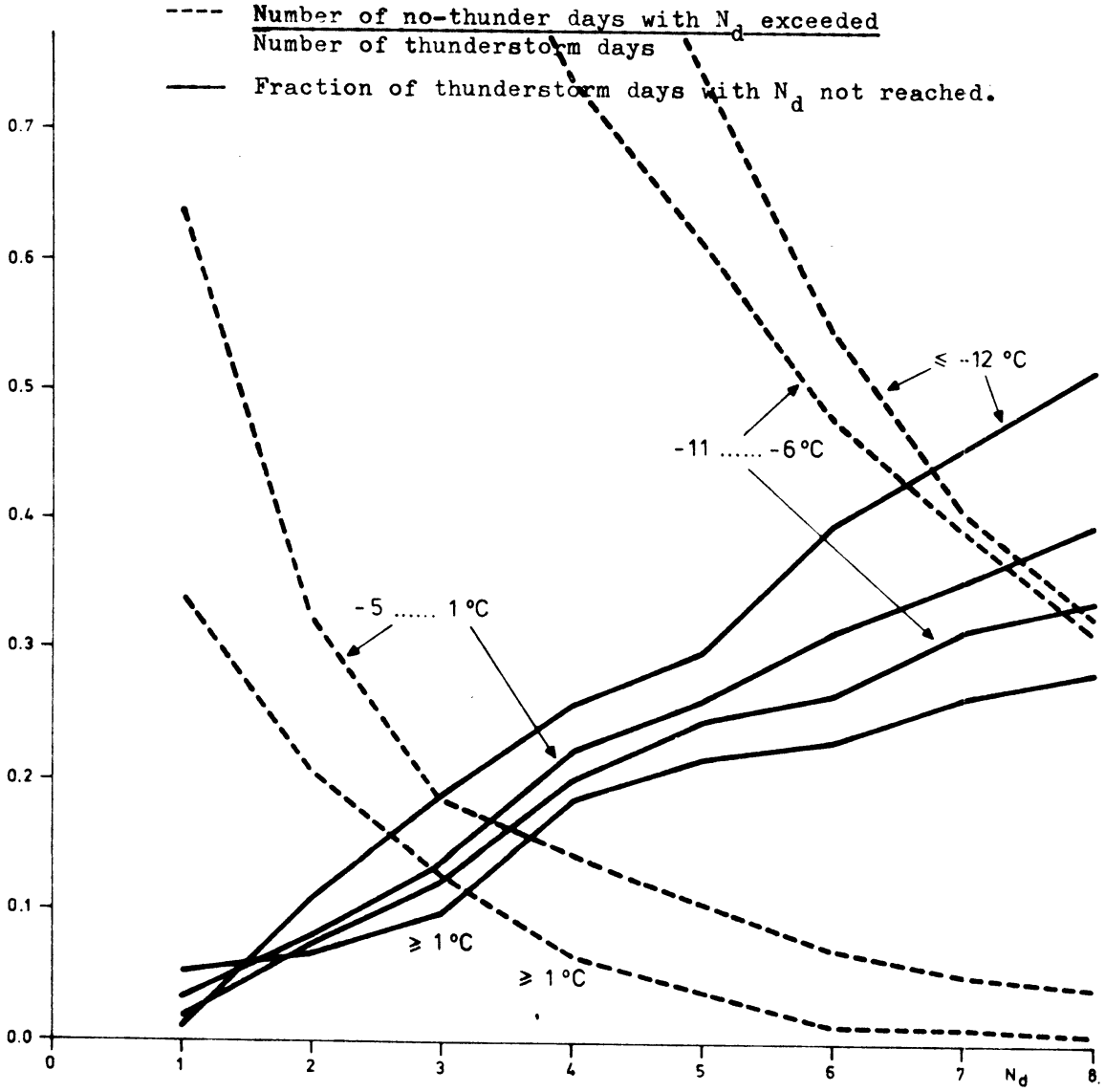

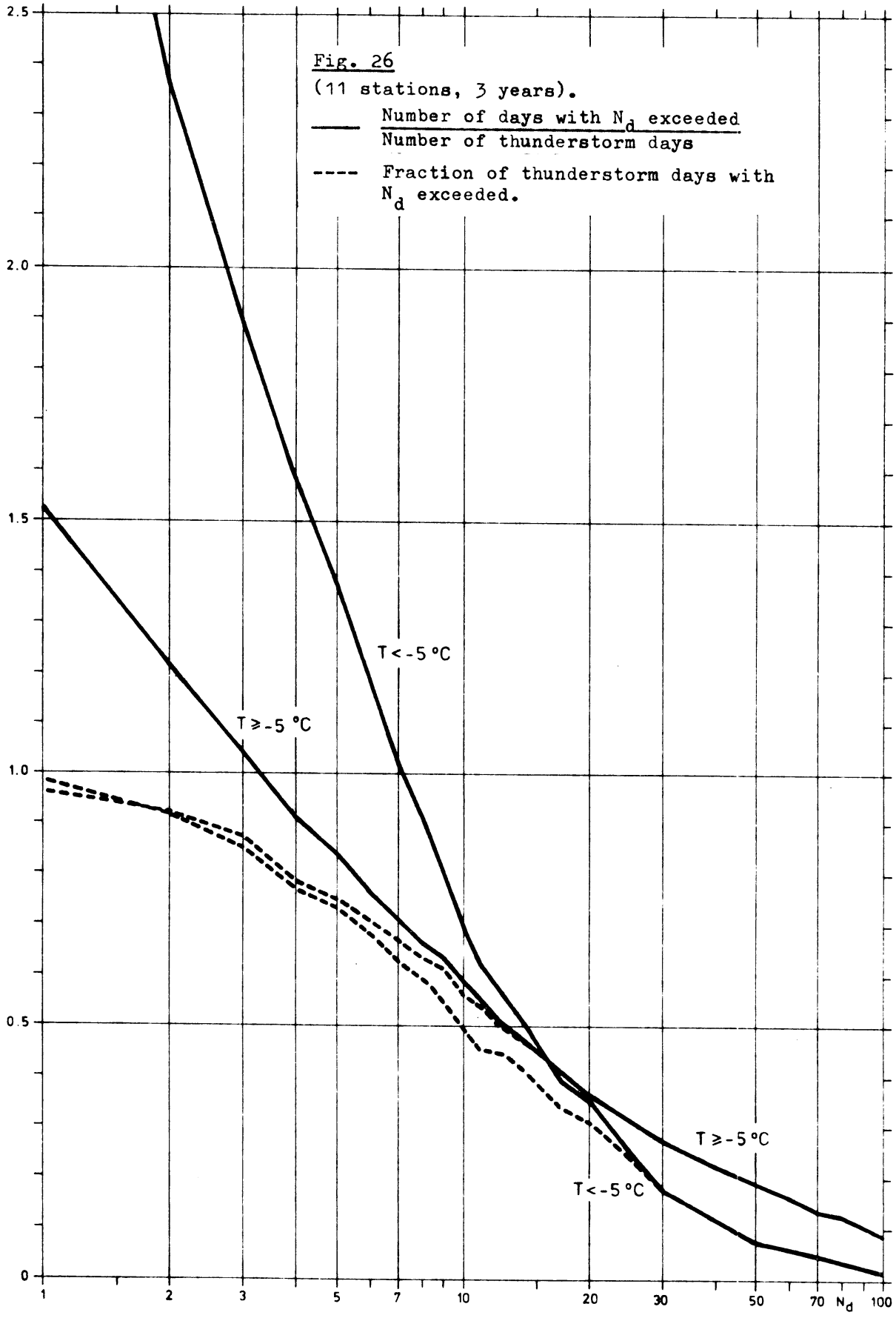
Fig. 26
(11 stations, 3 years).
Number of days with N_d exceeded / Number of thunderstorm days
Fraction of thunderstorm days with N_d exceeded.
T<-5 °C
T≥-5 °C
T≥-5 °C
T<-5 °C
2.5
2.0
1.5
1.0
0.5
0
1
2
3
5
7
10
20
30
50
70
N_d
100

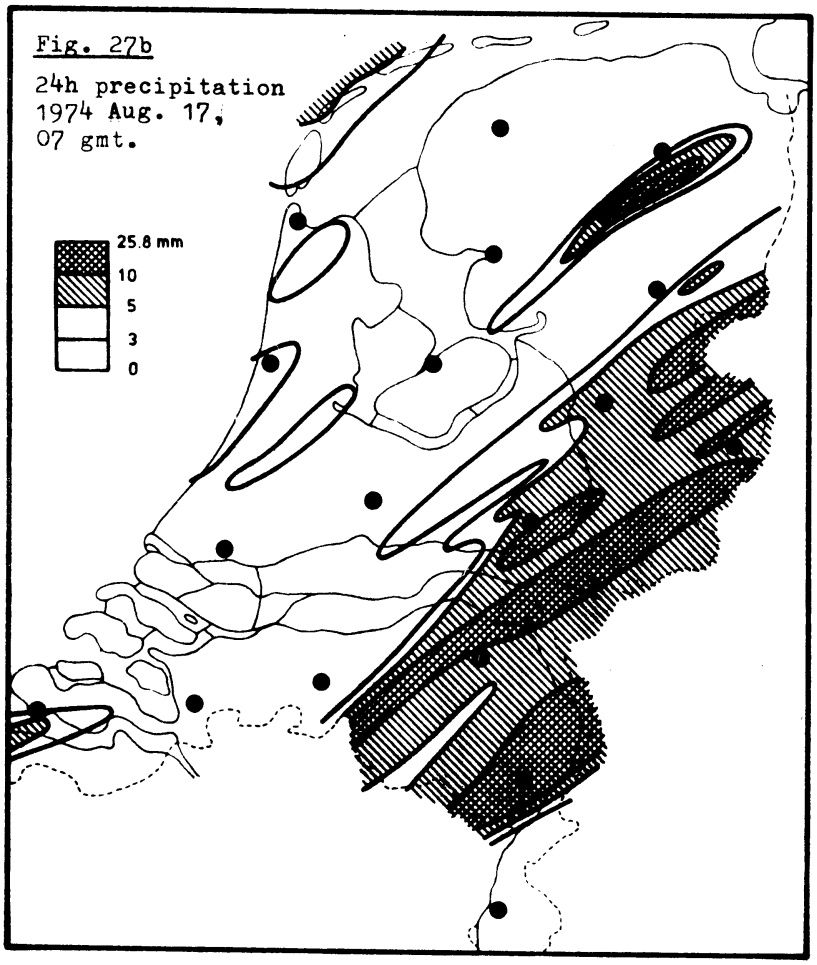

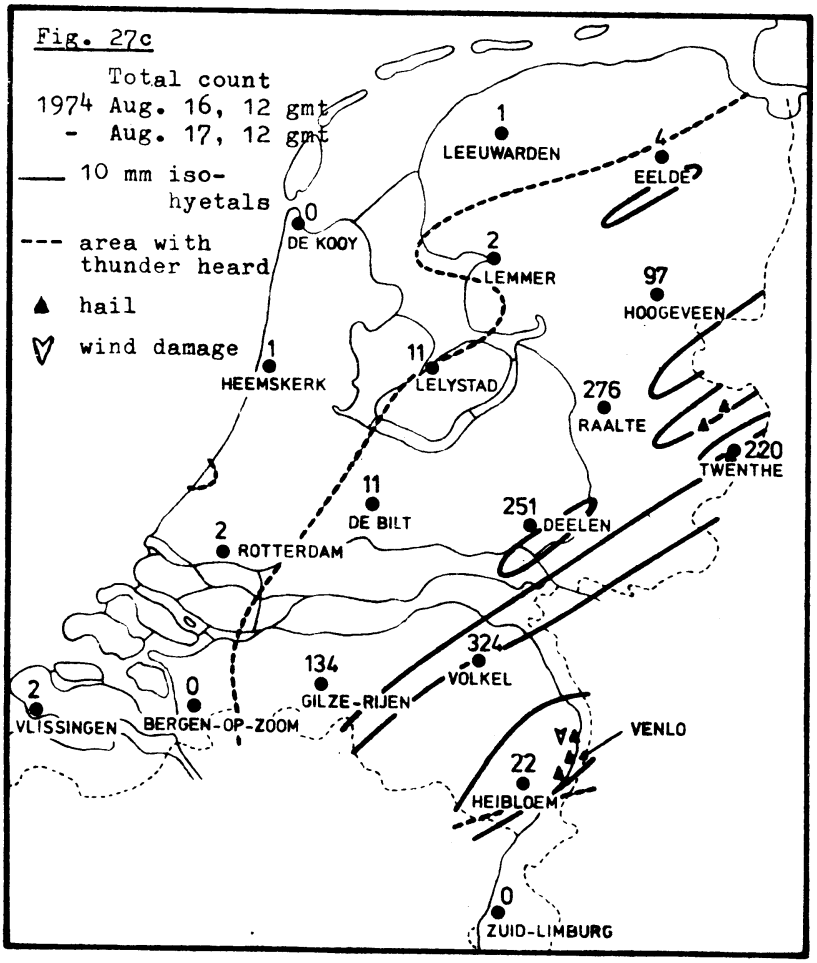

Fig. 27a

1974 Aug. 16/17 (10 min. counts)

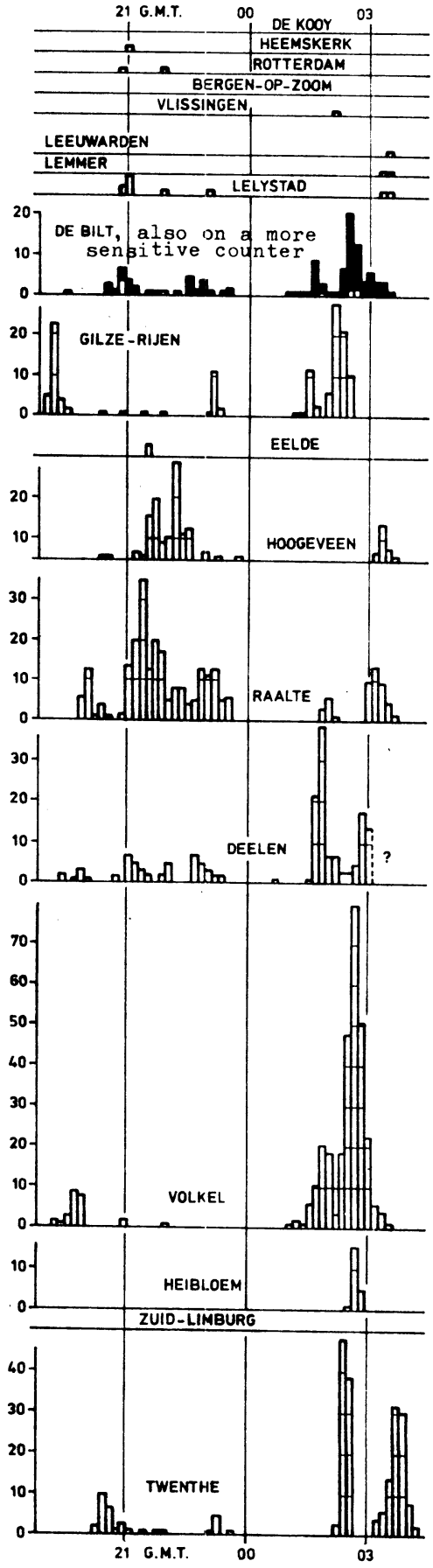

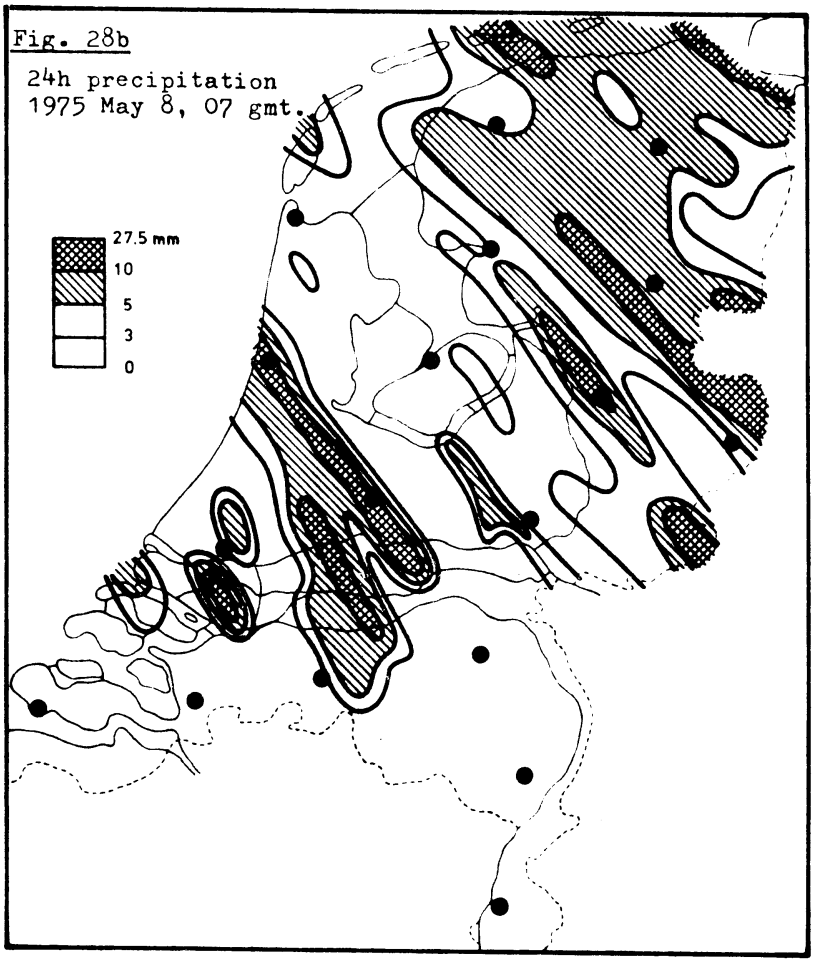

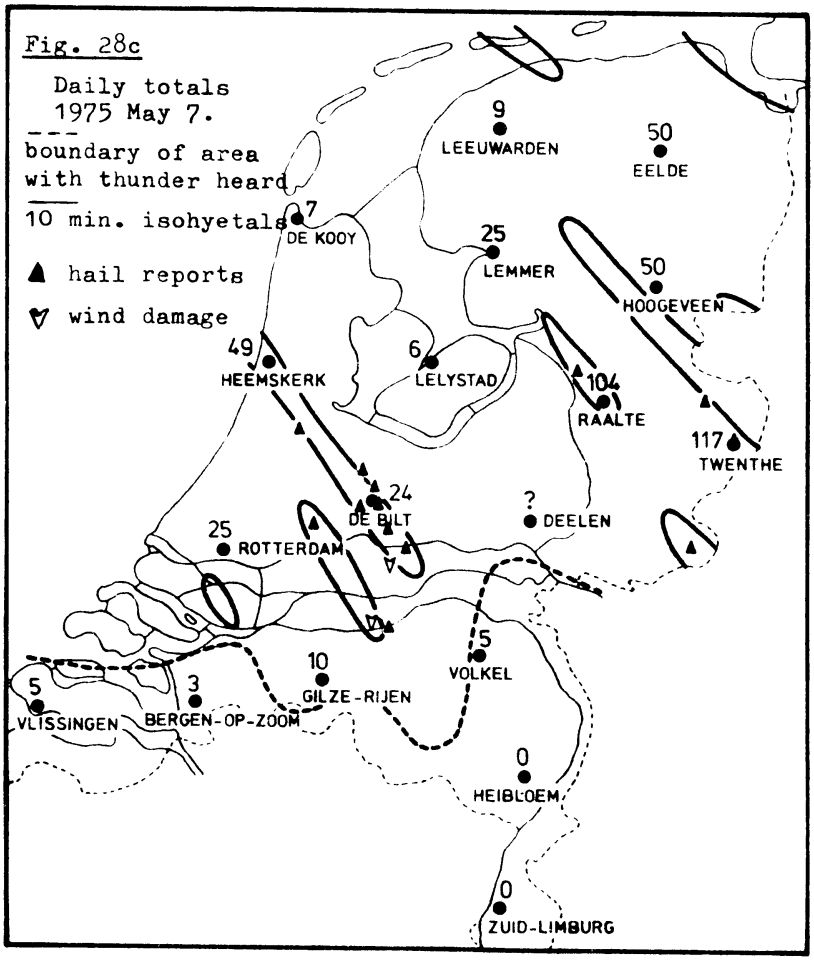

Fig. 28a 10 min. counts.
↓ 1975 May 7.

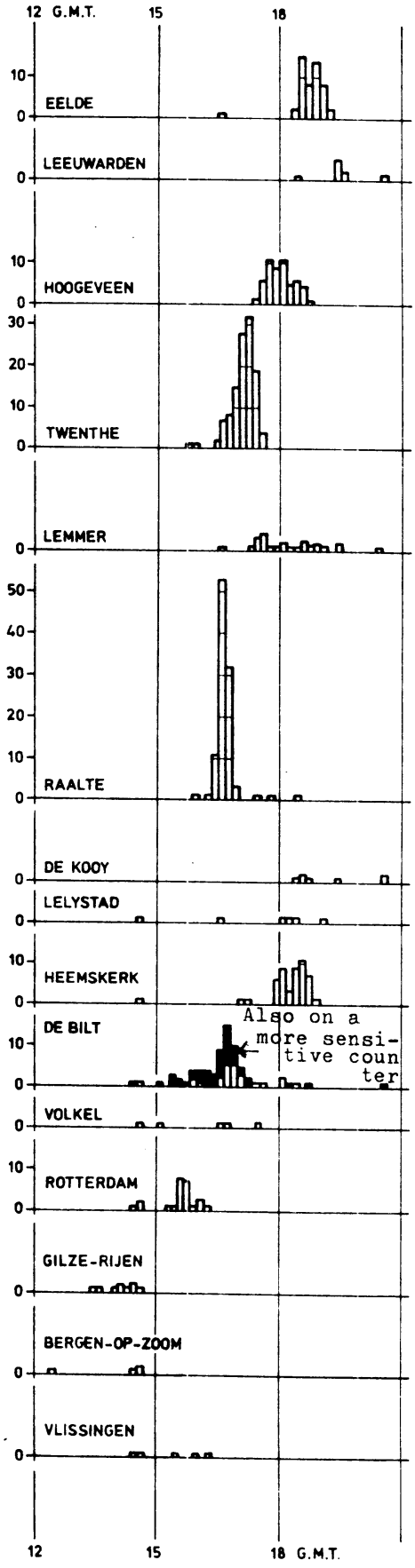

Fig. 29 Total counts for each station.

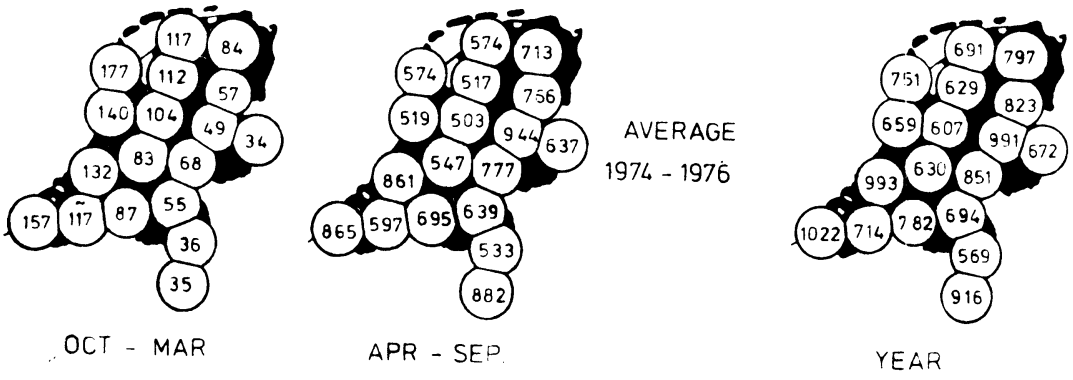

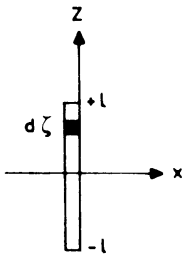

Fig. 30

Coordinates used in 10.1.

Fig. 31

Relative distortion of a vertical field as a function of the shape of an obstacle and the distance from that obstacle.

Full curves: ellipsoids;
dashed lines: cylinders.

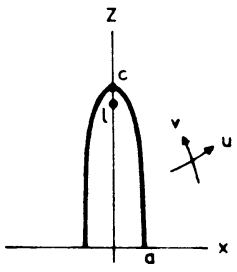

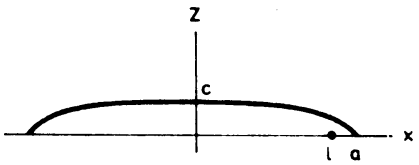

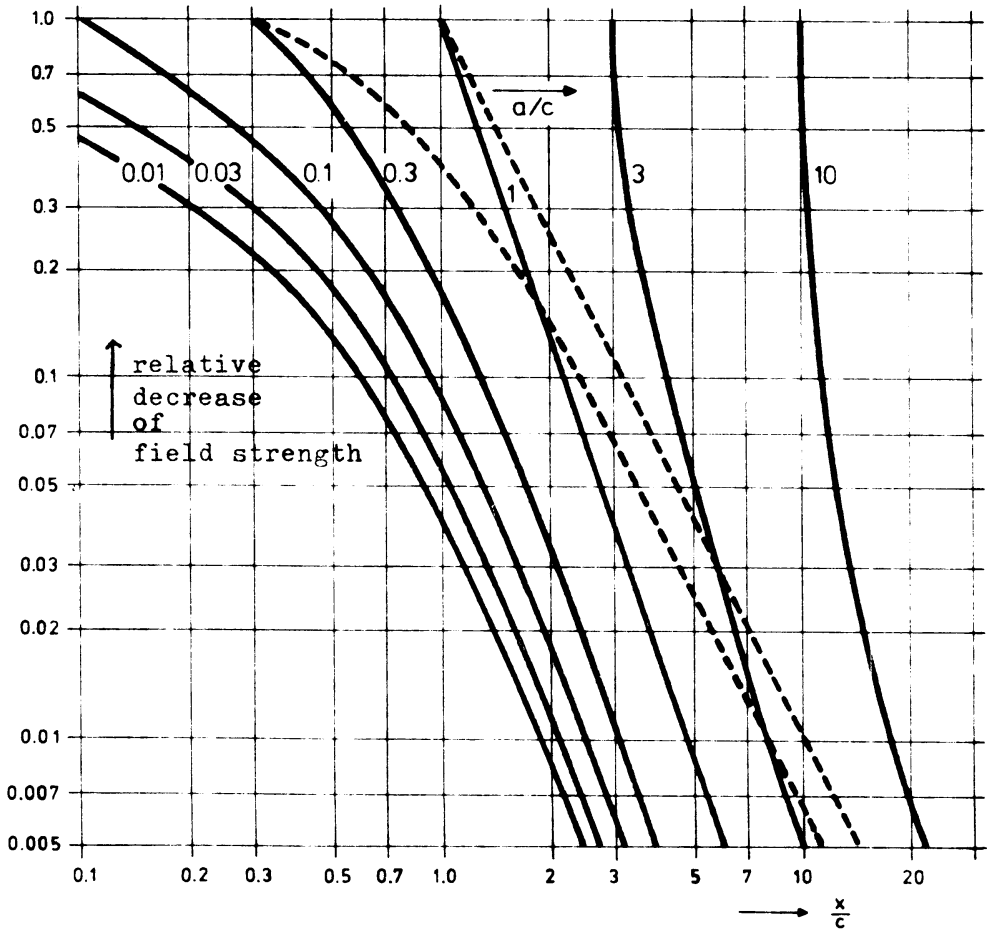

Fig. 32 Netherlands observer network 1956-1965.

Maximum flash frequency (reported from anywhere in the country) exceeded on the indicated percentage of thunderstorm days.